FACULTAD DE CIENCIAS DEL MAR

UNIVERSIDAD DE LAS PALMAS DE GRAN CANARIA

Guidelines for the interpretation of SAR images in the oceanic waters bathing Canary Islands

Candidate: Antonio Hernández Ballester

Advisors: Francisco José Machín Jiménez
and
Josep Coca Sáenz de Albéniz

Academic year 2018/2019

Trabajo fin de grado para la obtención del título de Graduado en Ciencias del Mar

FINAL DEGREE PROJECT – SIGNATURES SHEET

Title:

Guidelines for the interpretation of SAR images in the oceanic waters bathing Canary Islands

Academic year 2018/2019

Candidate:

Dr. Antonio Hernández Ballester
Faculty of Marine Sciences. ULPGC
antonio.hernandez122@alu.ulpgc.es

Advisors:

Dr. Francisco José Machín Jiménez
Department of Physics. ULPGC
francisco.machin@ulpgc.es

Dr. Josep Coca Sáenz de Albéniz
Robotics and Computational Oceanography Division. SIANI - ULPGC
jcoca@pesca.gi.ulpgc.es

Las Palmas de Gran Canaria, 14 de julio de 2019

Table of Contents

1. Introduction

This document summarizes the work carried on to produce the so-called 'Final Degree Project' required to obtain the Grade in Marine Sciences at the University of Las Palmas de Gran Canaria (taught in the Faculty of Marine Sciences).

It reports some basic research work done in the field of interpretation of imagery taken from spaceborne synthetic aperture radars[1] (SAR). The analyzed geographic region is constrained to the oceanic waters that bathe the Canarian archipelago. Accordingly, the starting point for this research is a set of SAR images (a representation of the roughness of the Earth surface, including the ocean) covering the year 2017 in full. These images are made available to the public through the internet within the framework of the Copernicus Programme[2], [1], [2], an initiative led by the European Commission in partnership with the European Space Agency (ESA).

From a technical point of view, a SAR image is a set of rasterized data. The values of the pixels represent the backscattering of the pulses emitted by the radar, which are caused by the roughness of the Earth's surface in the region covered. Therefore, a low value represents an almost flat area, while a high value is a rough one. On the surface of the ocean, in particular, many different phenomena or combinations of phenomena can cause the same pixel value or image features. Hence, understanding what is behind a particular oceanic SAR image is a challenging process that requires some expertise to do it, the image itself and a set of additional biogeophysical spatial data that we call here environmental data. This set of data include bathymetry of the area, sea surface temperature (SST), average wind intensity, chlorophyll-a concentration or a satellite image of the region in the visible and infrared portion of the electromagnetic spectrum, among others.

The Preface to our main reference, [3], points out the complexity of the topic in the following manner:

> *'Spaceborne synthetic aperture radar (SAR) provides a unique view of Earth's surface. The finely detailed imagery of the ocean's surface from SAR is assuredly the most complex and least understood data provided by remote sensing instruments. The sea surface can appear featureless or contain the signatures of such diverse phenomena as surface and internal waves, upwelling, current boundaries, shallow water*

[1] A radar is a detection system that, based on the comparison between transmitted and received electromagnetic radio waves, is capable to measure the size, position, or velocity of physical objects.

[2] Copernicus is an Earth observation programme that provides 'accurate, timely and easily accessible information to improve the management of the environment, understand and mitigate the effects of climate change and ensure civil security' [1].

bathymetry, wind, rainfall, roll vortices, convective cells, storms, and a wide variety of sea ice forms.' (C.R. Jackson and J.R. Apel, 2005)

In order to assist in the interpretation of SAR images in the Canarian Sea, it is of paramount interest to build up a catalogue of structures commonly observed in these waters. Consequently, the main objective of this work is to identify these structures from SAR imagery, analyze them and define a look-up table to be used as a guide in the interpretation of upcoming new images.

As mentioned in a previous paragraph, to achieve this, we have analyzed all available SAR images for 2017 in the selected geographical area. The images are free to download from ESA servers. Our analysis consists on:

a) Processing the image with SNAP[3], [4], a software specifically designed for the characterization of the images (it permits, for example, the measurement of distances, areas, wavelengths, etc., to select an appropriate colour palette to visualize the image or to perform a number of algebraic operations on pixel values).
b) Determine the state of the environment: to do this, the knowledge of environmental data is essential. In particular, of paramount interest are the average wind speed, along with SST, chlorophyll-a concentration and bathymetry of the area. Evenly important is to observe Quasi True Colour Images of the entire area, in order to have a synoptic view and infer the existing atmospheric situation. Obviously, their values are determined as close as possible to the moment when the SAR image was captured.
c) Use of guides available in the literature, [3], to identify the phenomena responsible for the observed effect.
d) Build the look-up table that contains the common structures in the region.

The structure of this document is as follows: Section 2 provides basic information on remote sensing and SAR, which will help to better understand the remaining sections. Section 3 briefly reports on the methodology followed to access all the required images and environmental data. It also explains in detail the proposed methodology to interpret SAR images. Section 4 summarizes the results obtained and describes the structures regularly found. Finally, Section 5 suggests some concluding remarks.

[3] SNAP is a computer program. The name stands for Sentinel Application Platform, it is a freeware offered by the European Space Agency designed to process and analyze images captured by the Sentinel satellite constellation [4].

2. Basic ideas on SAR Remote Sensing

The term remote sensing refers to any process capable of obtaining information from a physical entity in such a way that the measuring device (the sensor) does not come into physical contact with the entity itself. Satellite remote sensing, in particular, refers to data provided by sensors mounted on a space vehicle orbiting the Earth (in other words an artificial satellite, or more simply, a satellite).

One of the remote sensing technologies is radar that has grown because of number technical developments, [5]:

1. The ability of an antenna to emit an electromagnetic pulse in a precise direction.
2. The ability of an antenna to detect the attenuated echo scattered from a target, also with directional precision.
3. The ability of a system to measure the time delay between emission and detection and thus the range (distance perpendicular to the flight direction) to the target.
4. The ability to scan with the directional beam and so examine an extended area for targets.

The fifth advance has led to the development of SAR, as an evolved radar system. It has to do with signal processing, specifically, the application of spectral analysis to phase controlled signals. From the measurement of small Doppler shifts in signals from targets moving relative to the radar, it is possible to obtain good imaging resolutions, even from signals exhibiting small peak powers.

In this work, the sensor is an active sensor, a SAR, called C-SAR, in orbit around the Earth. The basic operation is as follows: C-SAR emits an electromagnetic signal from the orbit towards the Earth in a side-looking direction (to the right according to the direction of movement). The emitted beam scans the Earth surface (technical advance 4), covering in this manner a predefined area. For this, it is essential to have a thorough control of the propagation direction of the emitted wave and, consequently, a very accurate directional antenna is essential (technical advance 1). After a while, the antenna receives back a backscattered signal from Earth, the reflected signal or echo, (technical advance 2), that can be stored, processed and retransmitted to a base station on Earth. The comparison between the emitted signal and the received signal offers information about the time lapse between both signals (technical advance 3), the angle deviation (if any), power loss, Doppler (frequency deviation) and phase shift of the reflected signal. These and other parameters offer valuable information after some processing (technical advance 5).

C-SAR is an active sensor, this means that the device itself 'illuminates' (transmit pulses of microwave energy) the area to be analyzed. Therefore, it is possible to produce useful images without sun light. Besides, due to the properties of the electromagnetic propagation at the frequency band considered, the SAR image is clean because there is no interaction between the radiation and the atmosphere: the radiation used passes through the atmosphere without being modified (atmospheric gases, dust and clouds are transparent to it). In addition, depending on the frequency band used, it has low penetration coefficients in water, so we only observe surface disturbances of the oceanic area analyzed.

ESA puts in words this information by writing that the satellites are '*operating day and night performing C-band*[4] *synthetic aperture radar imaging, enabling them to acquire imagery regardless of the weather*', [6].

Remote sensing based on radar has advantages and disadvantages as compared with the more popular remote sensing at visible frequencies. Some advantages are:

- It operates in almost any weather condition.
- Day and night observation capability.
- Penetration through the cover of vegetation (depending on the frequency band).
- Penetration through the soil (depending on the frequency band).
- Small atmospheric effects (nearly negligible).
- Sensitivity to dielectric properties of the surface (e.g. frozen vs. liquid water).
- Sensitivity to the structure of surface components.

Among the disadvantages, we can cite:

- Difficulty to interpret the information (it is quite different from optical images).
- Presence of speckle (undesired salt and pepper effect in the images).
- Distortions in areas with marked topography (shadows, double bounce, etc.).

Finally, it is worth to say that remote sensing experts use to express that '*Someone's noise is another one's signal*', i.e. the information resides in tiny mixed-up signals.

2.1. The satellites: Copernicus's Sentinel-1 Mission.

We are using data from two spacecraft named Sentinel 1-A and Sentinel 1-B, launched in April 2014 and April 2016, respectively, by the ESA in the framework of the Copernicus Programme, [2]. Both satellites set up the so-called Sentinel-1 mission[5]. Sentinel 1-A and Sentinel 1-B circumnavigate the Earth in polar orbits sharing the same orbital plane.

The aim of Sentinel-1 mission is to capture images in C-band, being the radar carrier frequency 5.405 GHz, [8], corresponding to a wavelength of roughly 6 cm. It covers all

---

[4] A band of the electromagnetic spectrum from 4 to 8 GHz (3.75 to 7.5 cm wavelength), approximately.

[5] Each Sentinel-1 satellite is expected to operate for more than 7 years and have fuel on-board for 12 years, [6].

landmasses and, remarkably for our purpose, all coasts and the open ocean. The spatial resolution is down to 5 m, while the coverage may be up to 400 km.

Figure 1 shows a representation of one of the Sentinel-1 satellites. The total instrument mass is 945 kg, [8]. Three main parts catch our attention: two 10 m solar cell wings on the left and on the right (capable of producing 5,900 W), the central body hosting powering, storing/processing and communication equipment and, below the central body, the phased array antenna pointing to the Earth. The antenna represents most of the payload of the vehicle: it weighs 880 kg and is 12.3 m long and 0.82 m wide, [8].

Figure 1. Sentinel-1 (from https://bit.ly/2xwPqHR).

2.2. Basics on SAR imagery

The basic principle behind radar images is Fraunhoffer diffraction that models the along-track[6] resolution, Δa, of a radar instrument as directly proportional to the wavelength of the transmitted pulse, λ, and inversely proportional to aperture dimension (the length of the antenna in the along-track direction, L), [3]:

$$\Delta a \cong R \cdot \frac{\lambda}{L}$$

[6] The direction of flight path is defined as along-track or azimuth direction. The direction perpendicular to the flight path is the across-track or range direction.

R represents the slant range (the actual distance from the sensor to the object). Therefore, for a given wavelength the smaller the desired resolution, the larger the antenna.

On the other hand, the across-track resolution or range resolution, Δr, is given by, [3]:

$$\Delta r = \frac{c \cdot \tau}{2}$$

here c is the speed of light, and τ the pulse width (the pulse is a frequency modulated pulse). C-SAR exhibits a programmable pulse width in the interval [5, 100] μs.

When considering the wavelength, we have that for a radar sensor in orbit, a few tens of meters of resolution at visible and infrared wavelengths requires a camera aperture (this is, an antenna length in the azimuth direction, L) of only a few tens of centimetres. At microwave wavelengths, the same resolution would require antennas whose dimensions reach tens of kilometres. Obviously, this is not practical.

We have already pointed out the importance of having a directional antenna for radar operation in a previous paragraph. The practical solution for the suggested antenna problem (high directionality and practical length) is the implementation of active phased array antenna for SAR applications. Using this antenna the along-track resolution turns to be dependent only on the slant range, R, [3]:

$$\Delta a(SAR) = \frac{R}{2}$$

An active phased array antenna is an arrangement (a rectangular array) of single omnidirectional antennas assembled in such a way that the emitted waves interfere constructively or destructively in particular directions. As a result, it is possible to select a precise direction to guide the composed signal. Moreover, it is possible to control electronically the instant at which every single antenna of the array transmits the signal; this allows us to produce a beam capable of scanning the Earth's surface in certain angular interval (in both, along-track and across-track directions).

Now we can address the description of C-SAR sensor in ESA web page, [6]:

> *'The C-SAR instrument is an active phased array antenna providing fast scanning in elevation (…) and in azimuth (…). To meet the polarisation requirements, it has dual channel transmit and receive modules and H/V-polarised pairs of slotted waveguides.'*

The elevation here refers to the across-track direction where the sensor can direct the beam with an incidence angle interval from 20° to 46°, always to the right of the flight (there are four possible acquisition modes –see figure 3–, [6]). Regarding the along-track direction (azimuth) the angle may vary from -0.9° to +0.9°.

It has been reported, [3], that varying the polarizations of the transmitted signal and the received signal can help the interpretation of SAR images. That is the reason why C-SAR implements some control over the management of wave polarization. The sensor is able '*to transmit horizontal (H) or vertical (V) linear polarisations. The instrument is able to receive, on two separate receiving channels, both H and V signals simultaneously*', [8]. Therefore, there are a few combinations of available polarization schemes: HH for horizontal transmit and horizontal receive, or VV for vertical transmit and vertical receive. This simple case is called single-polarization. It is also possible to operate the radar on dual-polarization. In dual-polarization it is selected one polarization on transmit (H or V) and both on receive simultaneously. Hence, dual-polarization offers two images for every pass corresponding to HH-HV (HV for horizontal transmit and vertical receive), or to VV-VH (VH for vertical transmit and horizontal receive). Figure 2 illustrates these aspects. Both single-polarization schemes are outlined. On top of the figure is shown the VV scheme (vertical transmit and vertical receive) and, at the bottom, the horizontal transmit and horizontal receive (HH scheme).

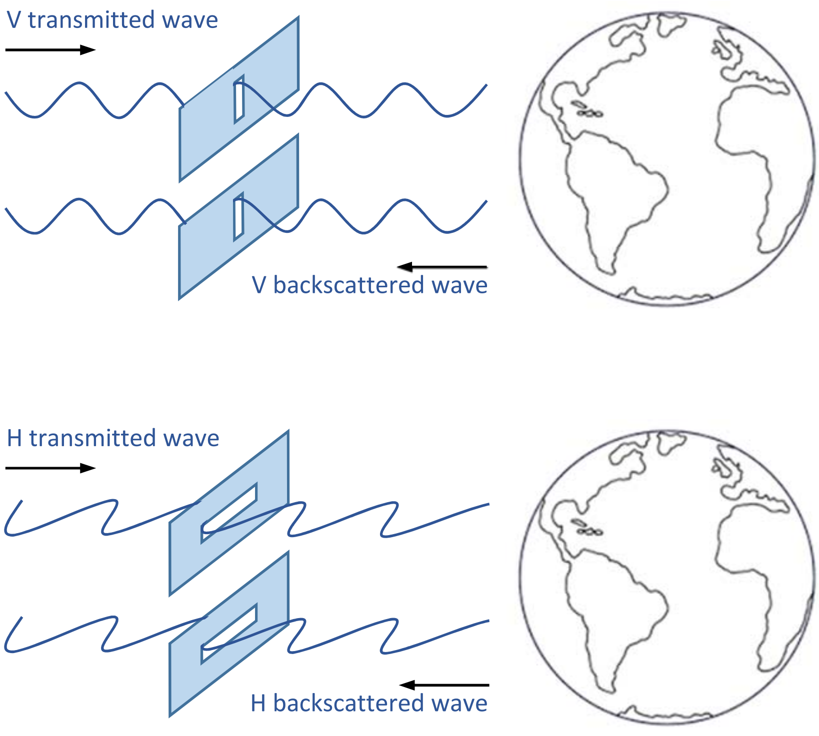

Figure 2. Single-polarization schemes. Top: VV scheme. Bottom: HH scheme. (Adapted from [7])

As a rule of thumb, the polarization scheme is used as follows, [6]: HH-HV or HH to monitor of the poles (sea-ice zones), and VV-VH or VV for all other observation areas.

2.3. Acquiring SAR images

This section is devoted to present the basic procedures followed to get an image of the Earth surface. Figure 3 shows the satellite in the four possible acquisition modes during its flight. It is travelling along the flight path (the direction defined by this path is the azimuth) at a uniform speed of around 7.5 km/s, and a roughly constant altitude close to 700 km (orbit height). Note, in figure 3, how the beam points down in the range direction, and it is directed towards the right side of the sensor. As mentioned in the previous subsection, the antenna performs an electronically controlled scanning in this direction. The scanning in the along-track direction (flight direction or azimuth direction) is due to its speed. The consequence of scanning both directions are the imaging of the regions coloured in yellow. These rectangles represent the scanned surface in every acquisition mode, and the composed area during the flight is referred to as the swath (the imaged surface). The side length in the direction perpendicular to the flight path (range direction) that is characterized by an incidence angle interval that varies from 20° to 46° depending on the particular acquisition mode (shown in the figure). The resolution of the modes are the following:

- Strip map (SM, provides coverage with a 5 m by 5 m resolution: high),
- Interferometric Wide swath (IW, 5 m by 20 m resolution: moderate),
- Extra-Wide swath (EW, 20 m by 40 m resolution: low), and
- Wave mode (WV, intended to determine the direction, wavelength and heights of waves on the open oceans).

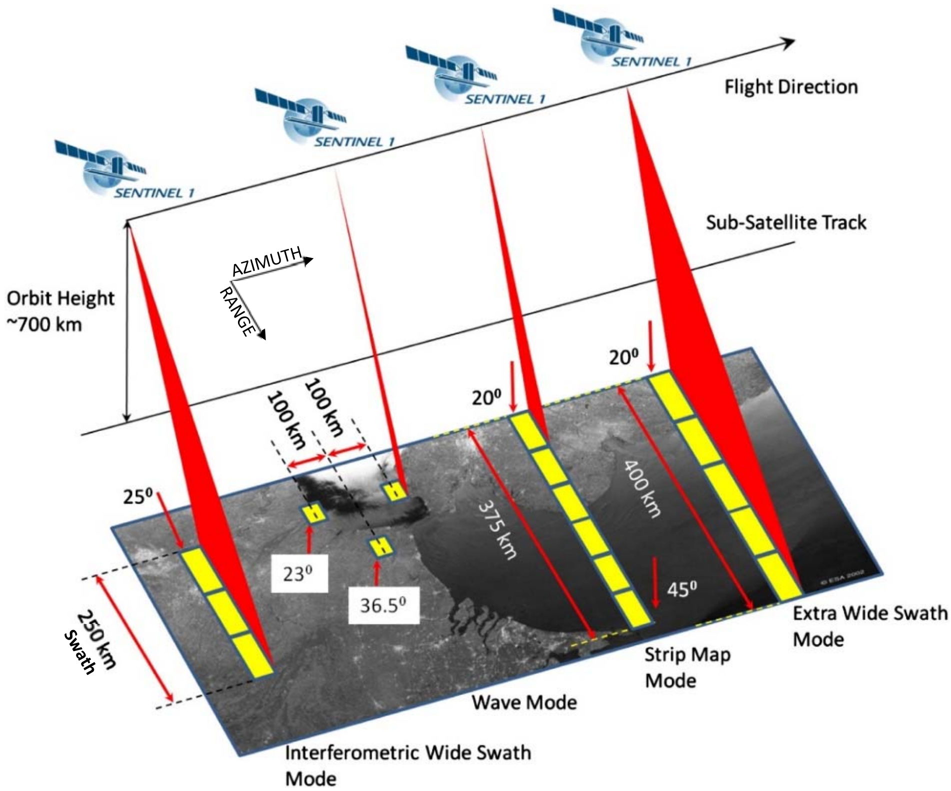

Figure 3. Scanning configuration for Sentinel-1. Acquisition modes (adapted from [6]).

The backscattered signal is then received from surface points at increasing range. Thus, digitizing the signal in time provides scanning in the range direction. The required digital processing is expensive in terms of CPU time.

It is worth to mention that the average times Sentinel-1A and Sentinel-1B passes over the region are 6:57:03$\pm$ 0:13:03 h and 19:04:02$\pm$ 0:09:02 h. This does not mean that we have two images every day, usually we only have one at any of those times. However, the same image taken in all passes is not exactly the same because there are spatial deviations. This last concept corresponds to the satellite revisit period (the time elapsed between observations of the same point on Earth). The revisit period is roughly 6 days.

3. Imagery acquisition and interpretation of SAR images

In this section, we are reporting details on the procedures to follow in order to attain the necessary data. As mentioned in the introduction two groups of data are needed: the images and the environmental data. Good quality images are obtained after downloading a number of files and intense computer processing. The environmental data requires similar procedures.

In a second subsection we present, in a step-by-step basis, the procedure followed to interpret a SAR image. From that procedure, we propose a methodology for the correct interpretation of the images.

3.1. Data acquisition: Imagery and environmental data

This work has been developed thanks to the availability of images and environmental data offered free to download by entities such as ESA and the National Aeronautics and Space Administration (NASA). The downloading method and the succeeding processing required before the images become useful deserves some comments. Likewise, the environmental data, i.e. bathymetry of the area, SST, average wind intensity, chlorophyll-a concentration or a satellite image of the region in the visible and infrared bands of the electromagnetic spectrum, must be collected and made available to the SAR images interpreter.

All the procedures presented in this subsection have been carried out by Dr. Josep Coca Sáenz de Albéniz in the Laboratory of ‘Teledetección’, assigned to the Robotics and Computational Oceanography Division of the University Institute SIANI (Spanish acronym for Intelligent Systems and Numerical Applications in Engineering) at the University of Las Palmas de Gran Canaria.

3.1.1. Sentinel imagery

The first step in obtaining SAR imagery is the selection of the desired products[7]. In particular, the chosen products were *Level-1 Ground Range Detected (GRD) Interferometric Wide swath mode (IW)* in 2017. This acquisition mode offers a large swath width of 250 km, and a moderate geometric resolution (5×20 m^2). The IW mode images three sub-swaths (see figure 3), the beam is electronically treated, [6], resulting in a higher quality image. To download the data from ESA website at the time it is made available, we run a batch process to download it. The routine that controls the transfer is coded with Python 3[8], and uses the standard module "sentinelsat". Sentinelsat makes searching, downloading and retrieving the metadata of Sentinel satellite images from the Copernicus Open Access Hub easily, [9]. The next phase requires the processing of the downloaded files. Sentinel 1 data processing is accomplished using SNAP, [4]. This program offers tools to perform certain tasks in console mode, which allows making calls to be run in batch mode.

A number of tasks must be performed prior to the use of images. We only mention the most relevant for our purpose: Thermal Noise Removal, Slice Assembly, Apply Orbit File, Calibration, Speckle-Filter, and Terrain Correction.

It is worth noting the possibility to modify the colour grey scale of SAR images using SNAP to improve their visualization. In this work, the typical interval for scaling the normalized radar cross section, σ^0, is [0, 0.06], unless otherwise stated.

3.1.2. Environmental data

We have already justified that these data are much needed for the interpretation of SAR images because environmental conditions determines the situation that is represented in the SAR image. We have already mentioned that these data include SST, average wind intensity, chlorophyll-a concentration or a satellite image of the region in the visible and infrared bands of the electromagnetic spectrum and bathymetry of the area.

Sea Surface Temperature (SST) and chlorophyll-a concentration

SST and chlorophyll-a concentration images are obtained after processing files downloaded from the NASA Ocean Colour Web[9]. The processing starts with data split in files corresponding to five minutes of acquisition of MODIS[10]. These files with five

---

[7] As denoted by the ESA.

[8] Python is a high level programming language: https://www.python.org/

[9] NASA Ocean Colour Web (OCW): https://oceancolor.gsfc.nasa.gov/

[10] MODIS (MODerate resolution Imaging Spectroradiometer) is a sensor operating in the visible band aboard the Terra and Aqua satellites.

minutes of acquisition are called granules, and are selected with the purpose of covering the region of interest. Using SeaDAS 7.5[11] the granules are treated to obtain SST and chlorophyll-a at full resolution. This includes some processing for geo-positioning and filtering of atmospheric noise, for that some auxiliary data are required. We manage one image per day.

Usually, the data acquired are post-processed to generate daily and five-day synthesis (five-day data combines two days before, the present day and two days later).

Wind data: speed and direction

The marine segment of the Copernicus European system[12] offers data for the wind calculation. In this case, the product selected is named '*Global Ocean Wind L4 Near real Time 6 hourly Observations*'. The wind is estimated from near real time scatterometer retrievals and from the analysis of the European Centre for Medium Weather Forecasts (ECMWF). We used data from three scatterometers:

- Advanced SCATterometer (ASCAT) aboard of Metop-A and Metop-B satellites from European Organisation for the Exploitation of Meteorological Satellites (EUMETSAT).
- OSCAT aboard of the Indian satellite OceanSat2.

The measured data include the backscatter coefficients and the associated radar parameters as well as wind retrievals. The results include the wind field at the synoptic times: 00:00, 06:00, 12:00, and 18:00 h UTC. The grid has a spatial resolution of 0.25° in longitude and latitude over global ocean. All the data are requested using the subsetting tools provided by the Copernicus marine segment[13].

Quasi True Colour images

Quasi true colour images for year 2017 (one image per day) are downloaded from the NASA's Earth Observing System Data and Information System [14] (EOSDIS) corresponding to two sensors MODIS[10], and Visible Infrared Imaging Radiometer Suite (VIIRS)[15].

We coded a Python 3 including functions from Global Imagery Browse Services[16] (GIBS) to automatically download the entire set of images, constrained to area of interest.

---

[11] A processing program called SeaWiFS Data Analysis System (SeaDAS): https://SeaDAS.gsfc.nasa.gov/

[12] marine.copernicus.eu

[13] http://marine.copernicus.eu/faq/what-are-the-motu-and-python-requirements/

[14] https://worldview.earthdata.nasa.gov/

[15] On board of the satellite Suomi National Polar-orbiting Partnership (SUOMI-NPP) operated by the United States National Oceanic and Atmospheric Administration (NOAA).

[16] https://wiki.earthdata.nasa.gov/display/GIBS/Map+Library+Usage

Bathymetry

These data is mainly needed near the coasts, where the islands' platform may influence the roughness of the sea surface (by means of an internal wave, for example). Sometimes it is also required in open waters.

Two sources of information are our main reference: a platform supported by the Autonomous Canary Government called Canary Islands Territorial Information System - Spatial Data Infrastructure of the Canary Islands[17] (IDE-Canarias), and Google Earth[18]

3.2. Looking at a SAR image

In section 2, we have presented some basic information on remote sensing and the production of SAR imagery from the technical point of view. In addition, in the last two subsections we have mentioned a good number of procedures required so that the end user may access the images with acceptable quality.

Figure 4 shows a SAR image taken on July 22nd, 2017 at 07:01 AM by the sensor C-SAR mounted in Sentinel-1B. Only Gran Canaria, Tenerife and La Gomera islands appear in the image, besides the Savage Islands, at the north.

We have to mention here that detecting something in a SAR image means that there is some backscattered signal. In imaging the surface of the ocean, this requires a certain roughness of the sea surface usually produced by the wind. Therefore, the wind intensity must exceed a lower bound, usually 2 m/s. Otherwise, the corresponding pixel value would be negligible.

Our initial knowledge is that the dark areas (low pixel values) represent almost flat areas, while clear areas (high pixel values) are rough ones. Thus, we can say that the lands areas display much higher roughness than the oceanic areas. Moreover, the surface of the ocean is more irregular at the east than at the northwest of the image. Clearly, at the south/southwest of the three Islands, there are still zones, maybe due to the protection every island offer to the wind presumably blowing from the northeast (this point should be confirmed). In addition, some kind of von Karman vortex streets seem to appear in the southern areas.

The remaining information contained in the image is hidden: there are 'shadows' similar to clouds at the north, though in the image we do not have any representation of the clouds because they are transparent to our radiation. If there are clouds in the area, maybe there is some atmospheric/ocean interaction to be confirmed. As well, there is a

---

[17] https://visor.grafcan.es/visorweb/#

[18] https://www.google.com/earth/

figure in the southwest direction from Gran Canaria (some kind of twisting shadow) that could be interpreted as altered von Karman streets.

First, we should try to verify our assumption regarding the wind direction. We need more information to do that. One of the data we have collected with our Environmental pack is the spatial distribution of the average wind speed at different hours. In particular, we have the representation of the average wind velocity field in the area at 6:00 AM shown in figure 5.

Figure 4. Sentinel-1B fine resolution SAR image taken on July 22nd, 2017.

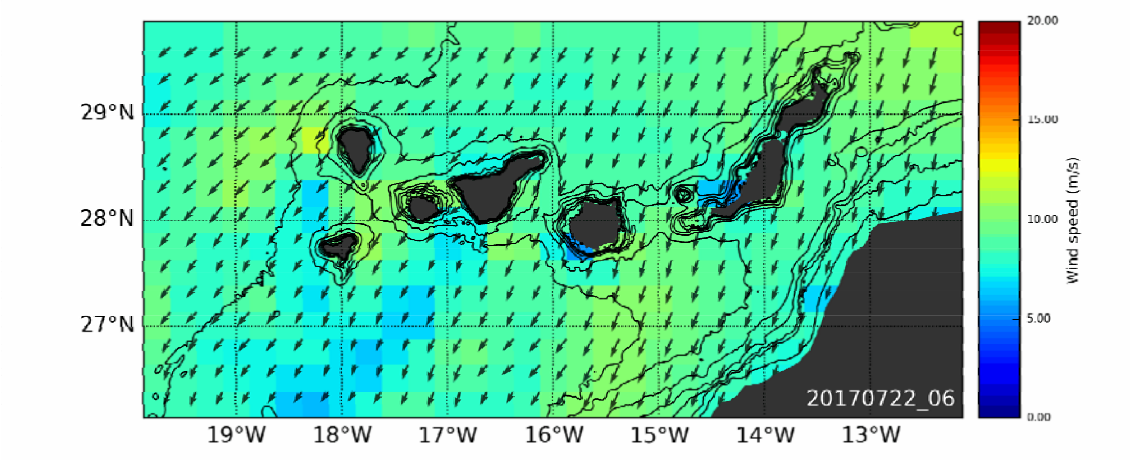

Figure 5. Average wind velocity field in the area on July 22nd, 2017 at 6:00 AM.

It is evident, form figure 5, that the wind blows as expected in the region analyzed: it comes from the north/northeast with a moderate intensity at the north (10 m/s) and low intensity (5 m/s) close to the south/southwest of the islands. In addition, at the east of Gran Canaria it is stronger than at any other zone of the image (about 12 m/s). This would explain the intensified roughness measured.

To make a step forward in the interpretation of the image we need more information. Figures 6, 7 and 8 show quasi-true colour satellite images of the area on July 22nd, 2017. Figure 6 is the capture of sensor MODIS travelling on board of satellite Terra. There is a heavy cloud cover at the north of the image.

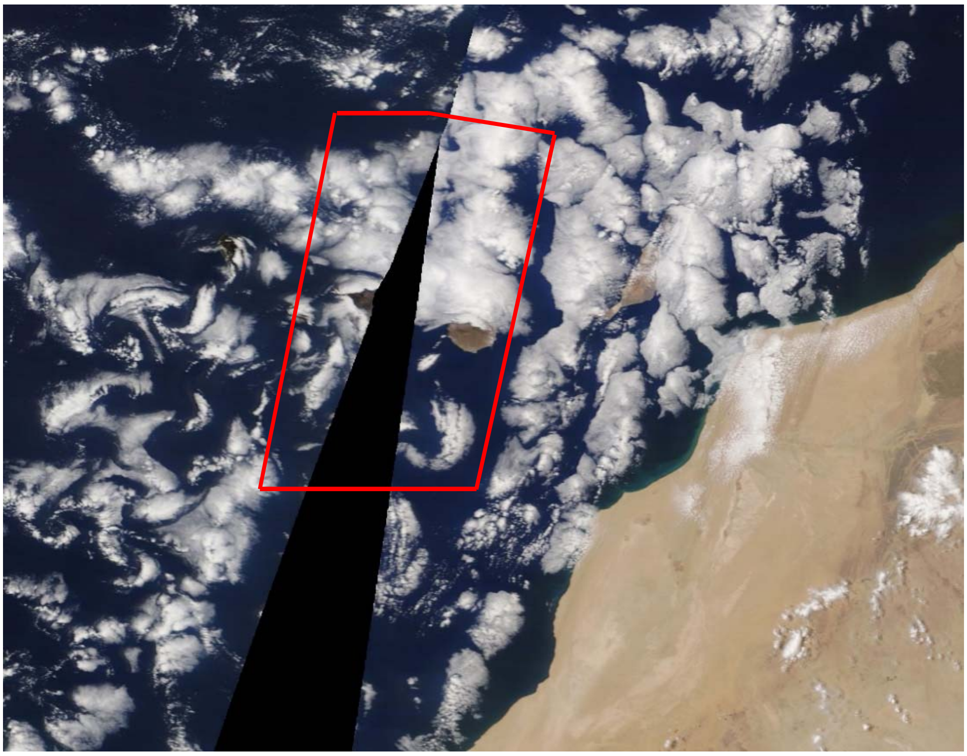

Figure 6. MODIS aboard of Terra image of the area on July 22nd, 2017

Figure 7 displays the image acquired with sensor VIIRS aboard of Suomi NPP. Clearly, this image has been taken later in time and the cloud cover is dissipating. Finally, figure 8 represents the image obtained with sensor MODIS aboard of Aqua. This third image is quite similar to that in figure 7. There is a red box indicating the approximate boundary of our SAR image in figure 4.

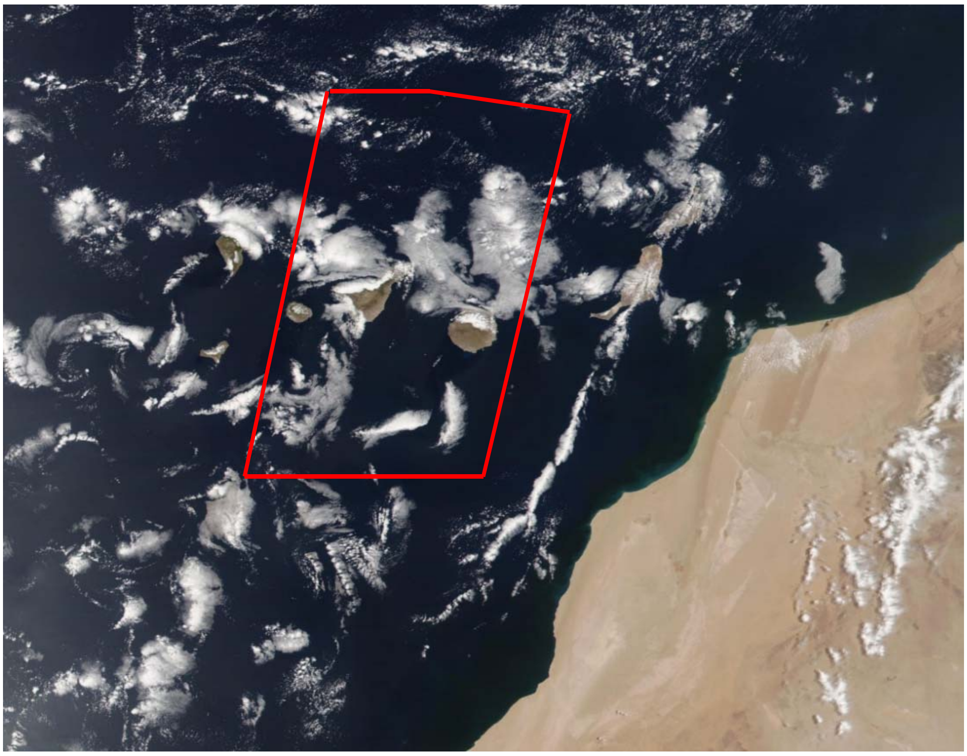

Figure 7. SNPP-VIIRS image of the area on July 22nd, 2017

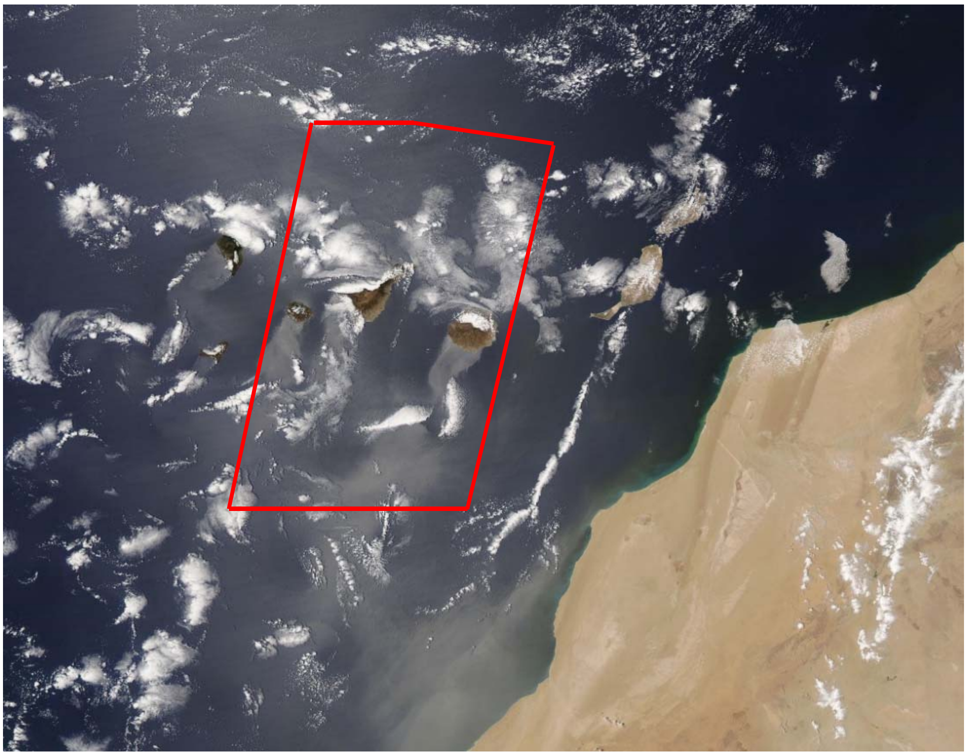

Figure 8. MODIS aboard of Aqua image of the area on July 22nd, 2017

These three images were captured in sequence: Terra passed over the region before Suomi NPP, and this satellite before Aqua. Our SAR image and the image in figure 6 were captured at similar instants, and the roughness of the sea surface is related, somehow, to the heavy cloud cover at the north of the area observed.

The need of the sea surface temperature (not in this example case) is justified to characterize the weather conditions. Moreover, together with SST chlorophyll-a concentration is also significant when exploring the change in roughness (usually a reduction) due to the presence of primary producers suspended in the photic layer of the ocean. This biomass produces surfactants that modifies the surface tension.

Figure 9 is a zoom of the central region of the image in figure 4. Note the lines more or less regularly spaced in the direction NE-SW between the islands (see encircled area). With a doubled headed yellow arrow, we indicate the direction of the wind in that area. Clearly, both the lines regularly spaced and the wind share directions.

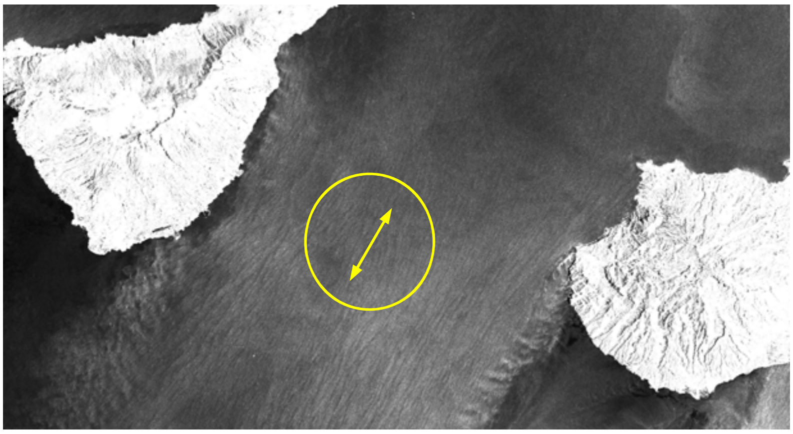

Figure 9. Zoom of the central region of the image in figure 4.

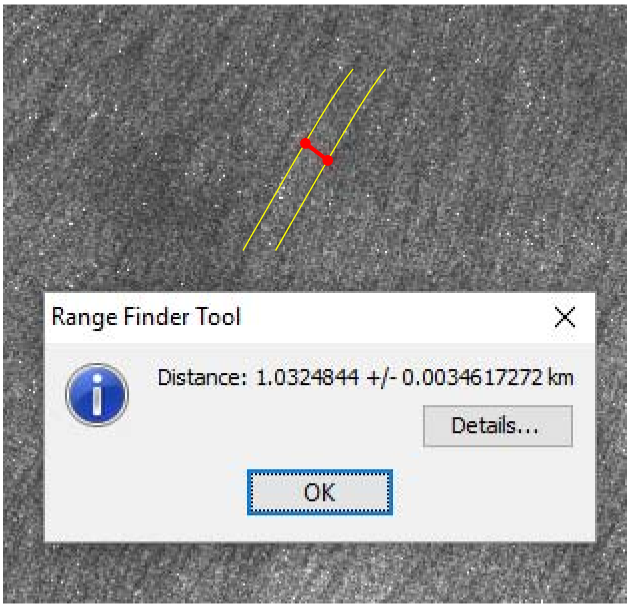

Figure 10. Using SNAP, [4], to estimate wavelengths.

We have already pointed out that SNAP provides functions to measure distances. Therefore, we can determine the wavelength of the phenomenon as figure 10 illustrates. There we show a zoom of the zoomed area in figure 9. In yellow, we emphasize two of the lines regularly spaced and use SNAP to measure the resulting wavelength. As displayed, the resulting parameter is roughly 1.0 km.

There are tools in the literature that provides assistance in taking steps forward in our analysis. Table I is an example of such a tool. The first column lists the oceanic phenomena that may be observed in the SAR images: surface waves, internal waves, internal tides, currents and fronts, eddies and alterations associated with bathymetry in shallow waters. For every phenomena, the second column indicates the spatial parameter that characterizes it. The third column, on the other hand, details the physical quantities measurable from the image. The fourth indicates the physical mechanism that produces the variation of the roughness of the surface, while the fifth column defines the typical wind speed that conditions that the phenomenon is visible in the SAR images, provided it is present in the area with the specified intensity interval. Observe how, as mention at the beginning of this subsection, the wind speed must exceed some lower bound value in all cases. The last column describes some properties of each phenomenon.

Tables II and III show, with a similar structure, the interactions between the ocean and the atmosphere that can be determined with the images, namely: winds at sea level, vortices, gravitational waves and rain cells. Table III reports the characteristics of the surface of the ocean when surfactant films or mineral oils appear, both of organic origin.

In addition to the above, it is very common to observe wakes of ships whose propellers create zones of convergence/divergence that modify the roughness of the marine surface, reaching lengths of several tens of kilometres.

Returning to figure 9, we wonder if the lines regularly spaced are a manifestation of roll vortices (also called windrows, see table II). This assumption is sensible because that phenomenon fits with our observations: the measured wavelength of 1 km fits the given interval (column 2), the speed is 12 m/s (it belongs to the interval in column 5), and the velocity of the wind is parallel to the pattern observed (column 6). Consequently, we can confirm that we are observing roll vortices, unless otherwise stated.

Table I. Ocean Features on SAR Imagery (copied nearly 'as is' from [3], [10])

Feature	Scale (km)	Derived Measurement	Imaging Mechanism	Wind Speed Range ($m \cdot s^{-1}$)	Remarks
Surface Waves	Wavelength [0.1; 0.6]	– Wavelength – Propagation direction – Wave height	– Tilt Hydrodynamic Velocity – Bunching	[3; 40]	(1)
Internal Waves	Wavelength [0.3; 3]	– Wavelength – Direction – Amplitude – Mixed layer depth	– Convergence/Divergence – Surfactants	[2; 10]	(2)
Internal Tides	[10; 20]	– Wavelength – Direction	– Interaction of centimeter: waves, currents or surfactants	[3; 7]	
Currents and Fronts	[1; 100]	– Location – Shear – Strain – Velocity	– Shear/Convergence – Convergence – Wind Stress – Surfactants	[3; 10] [3; 10] [3; 10] [3; 7]	(3)
Eddies	Diameter [1, 200]	– Location and source – Diameter – Velocity Shear – Strain	– Shear/Convergence – Wind Stress – Surfactants	[3; 10] [3; 10] [3; 7]	(3)
Shallow Water Bathymetry	Depth [100, 600]	– Location/change detection – Current velocity – Depth	– Convergence	[3; 12]	(4)

(1) Azimuth-traveling waves may be nonlinear without correction. Other limiting factors include wavelength, wave height and fetch.
(2) Curvilinear packets with multiple waves, decreasing wavelength from front to back. Sensitive to wind conditions, wave crest orientation to platform.
(3) Sensitive to wind conditions. Often multiple mechanisms present simultaneously.
(4) Sensitive to wind, current properties and depth.

Table II. Air-Sea Interactions on SAR Imagery (copied nearly 'as is' from [3], [10])

Feature	Scale (km)	Derived Measurement	Imaging Mechanism	Wind Speed Range ($m \cdot s^{-1}$)	Remarks
Surface Winds	Grid > 1	– Wind speed – Wind direction	– Wind stress – Indirectly via windrows, models, or sensors	[3; 25]	(1)
Roll Vortices	Wavelength [1; 5]	– Boundary Layer: stratification	– Wind stress	[3; 15]	(2)
Gravity Waves	Wavelength [2; 10]	– Height – Turbulence spectrum – Drag Coefficient	– Wind stress	[3; 15]	(3)
Rain Cells	Diameter [2; 40]	– Rain rate	– Wind stress – Rain damping	[3; 15]	(4)

(1) For mesoscale, coastal variability. Requires good calibration.
(2) Long axis/crests parallel to wind direction.
(3) Long axis/crests perpendicular to wind direction, often associated with topography.
(4) Appearance sensitive to frequency, rain rate, wind speed.

Table III. Surface Films on SAR Imagery (copied nearly 'as is' from [3], [10])

Feature	Scale (m^2)	Derived Measurement	Imaging Mechanism	Wind Speed Range ($m \cdot s^{-1}$)	Remarks
Biogenic Surfactants	Area > 100	– Areal extent	– Convergence	[2; 8]	(1)
Mineral Oils	Area > 100	– Areal extent	– Seeps – Ships discharge – Run-off	[3; 15]	(2)

(1) Both forms have signatures similar to low wind, cold thermal water masses, etc.
(2) Win speed, combination of L- and C/X-bands may enable discrimination of each form.

3.3. Interpretation of fine resolution SAR images

Therefore, to interpret a SAR image, we analyse all the available environmental information and the SAR image is observed in detail in order to:

- Identify the possible recognizable patterns: this is done recognizing the spatial arrangement of the pixels.
- Measure, using SNAP, relevant parameters such as the wavelengths in those structures that have a spatial periodicity. The parameters, together with environmental data, can characterize a specific phenomenon. In many other cases it is not possible to determine the cause-effect relationship in the image and it is a failed interpretation.

Use tables I, II and III to check which ocean feature, air-sea interaction or surface film is responsible for the pattern.

We have pursued this methodology of analysis with the SAR images of the year 2017. As a conclusion we have found that the following structures are observable with certain regularity in our region of interest (the oceanic waters bathing Canary Islands):

- Surface waves (observation of waves is very common).
- Internal waves.
- Eddies.
- Windrows or roll vortices.
- Rain cells.
- Gravity waves.
- Eddies associated to von Karman streets.
- Biogenic surfactants.
- Oil stains.
- Ship wakes.

Marked with ^{O} are the features associated with a pure oceanographic trigger. An asterisk (*) means that they are the phenomenon due to air-sea interactions.

In addition, there are algorithms that compute surface wind speeds from SAR images. However, they lack accuracy when the intensity is low.

The following section presents examples of all this patterns, these examples constitute the desired look-up table.

4. Results

This section reports the results of the work. It is worth to mention that the success of it requires training the eyes so that they (the eyes) become familiar with the grey images. Only after a while, we begin to discover that SAR images are full of textures and are colourful, somehow.

We have applied the methodology described in the previous section to detect patterns from the SAR images and, from them attempt to give a possible cause from what is contained in tables I, II and III. We want to emphasize that reference [3] is of paramount importance for our developments.

In the following subsections, we include one or two images corresponding to a physical phenomenon encountered regularly in the region of interest. We restrict our analysis to those physical causes listed at the end of the previous section. In any case, we make an effort to justify the particular physical mechanism involved, when this is possible in simple words.

Therefore, the SAR images that follows want to be representative of the observations, so that the promised look-up table are the images itself. The images are intended to be used as a humble reference for beginners.

4.1. Ocean features.

We are following the same nomenclature as in reference [3], so, this subsection describes those patterns in the images due to oceanographic properties.

4.1.1. Surface waves.

Surface waves are a very common observation in any superficial mass of water. The most common group of surface waves arrives our costs as swell. It is well known that swell is produced by a distant wind blowing at an approximately constant velocity. The SAR image of a surface wave is brighter than the average backscattering in the crest and darker in the trough.

The record of these waves in SAR images is much clearer than images from any other sensor mounted in a satellite.

Obviously, we observe surface waves frequently in the water around Canary Islands. When the intensity of the wind is moderate or low, we observe a pattern similar to the one presented in figure 11. The entire region in the SAR image is full of lines corresponding to crests of waves moving toward the east. Note how the north of Tenerife produce observable refractions. Encircle in yellow are four ships, allegedly oil platforms.

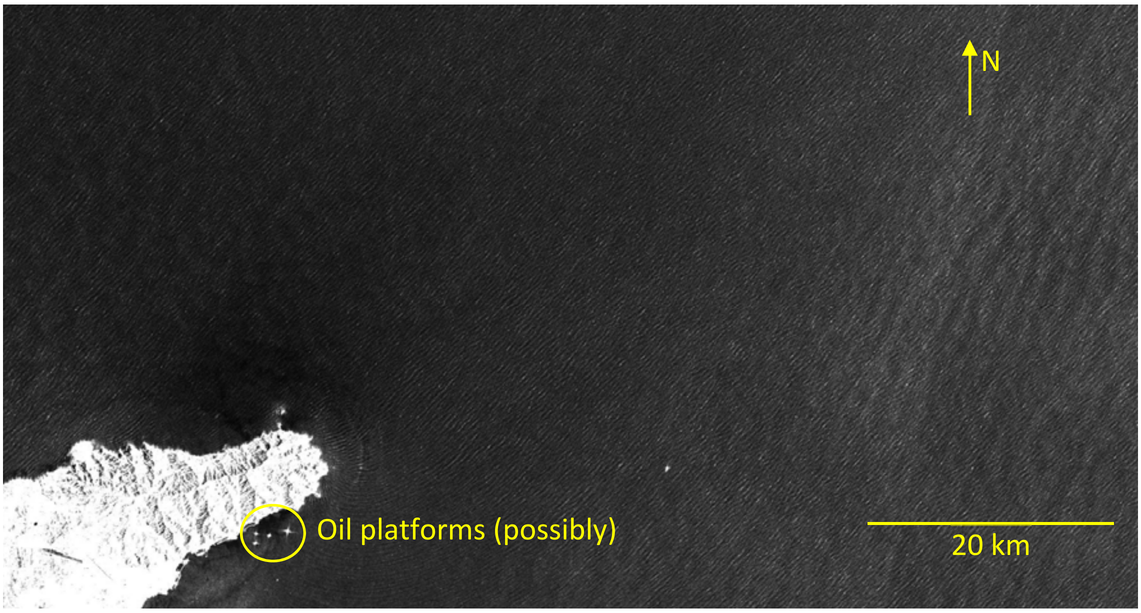

Figure 11. SAR image captured on March 30th, 2017. Surface waves.

4.1.2. Internal waves.

Internal waves appear in stratified waters. These waves are gravity waves that propagate within the water and not on the surface. They enhance mixing and the availability of nutrients at surface waters. Internal waves usually seen on SAR images form along the stratified seasonal thermocline, below the upper mixed layer. Tidal forces usually generate them over abrupt topographies. They are observed in SAR images due to interactions between the current field and surface waves driven by the wind field.

Internal waves materialize as packets (groups of waves). The waves present curvilinear crests and the wavelength decrease to the back of the packet. They appear as a sequence of bright bands (the convergence zone that accumulates surfactants) followed by a dark band (divergence part).

Dealing with our observations, on one hand, we have the figure 12 that regards with the abrupt topography matter: The yellow path represented is 36.5 km long, and the depth along it varies more than 1,000 m. That is a considerable variation, suggesting the approximate position of the continental slope of Africa there.

On the other hand, the SAR image we have selected was obtained on July 12th. That day the wind speed was moderate to low about 6 or 7 m/s (at 6:00 AM, the closest time to that of the image was taken, 6:44 AM), blowing from the north in that segment of the Africa coast considered. Figure 13 presents the SAR image (Internal waves have been detected at wind speeds between 2 and 10 m/s). Note how the continental slope and the beginning of the curving structures nearly coincides suggesting some kind of connection between both effects.

Figure 12. Google Earth© image showing the continental slope (dashed line). The depth changes 1,100 m in about 36.5 km (from Google Earth).

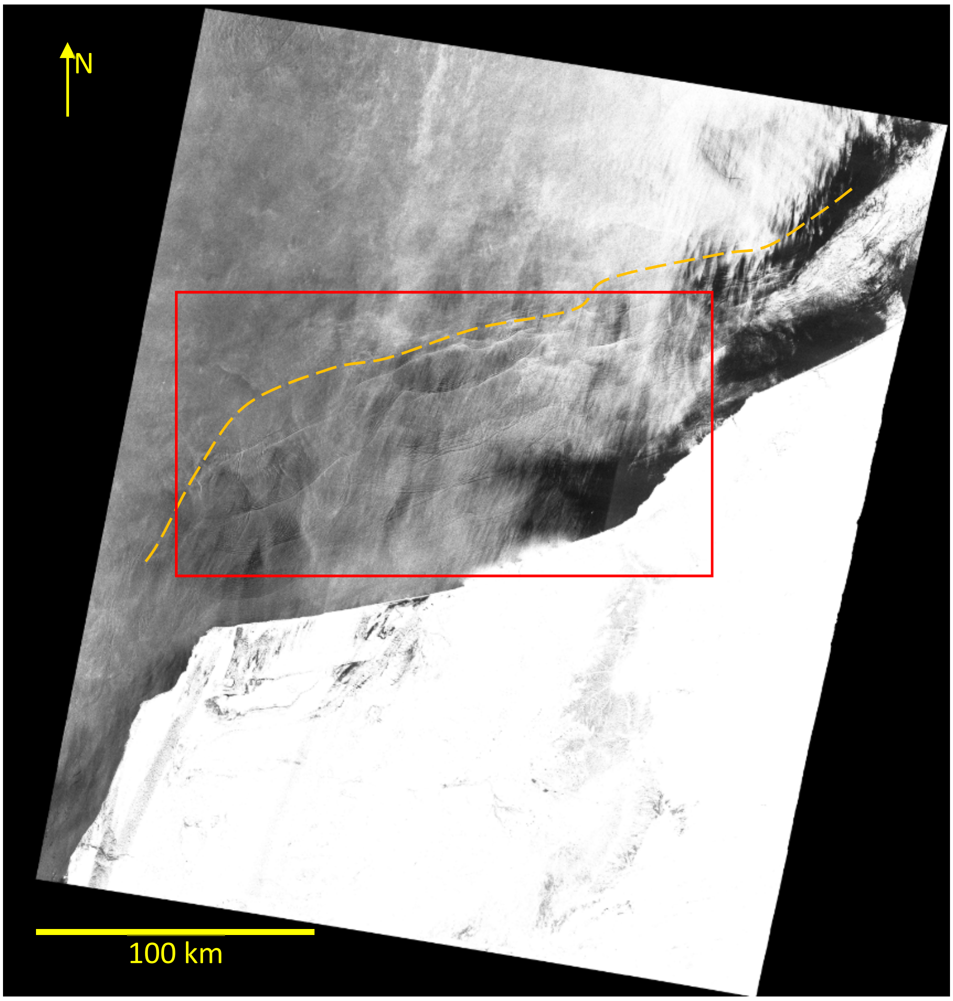

Figure 13. SAR image captured on July 12th, 2017. Internal waves. (Grey scaling: [0, 0.03])

Trains of waves compose the pattern. To characterize them we have included figures 14 and 15 zooming the original image included in figure 13.

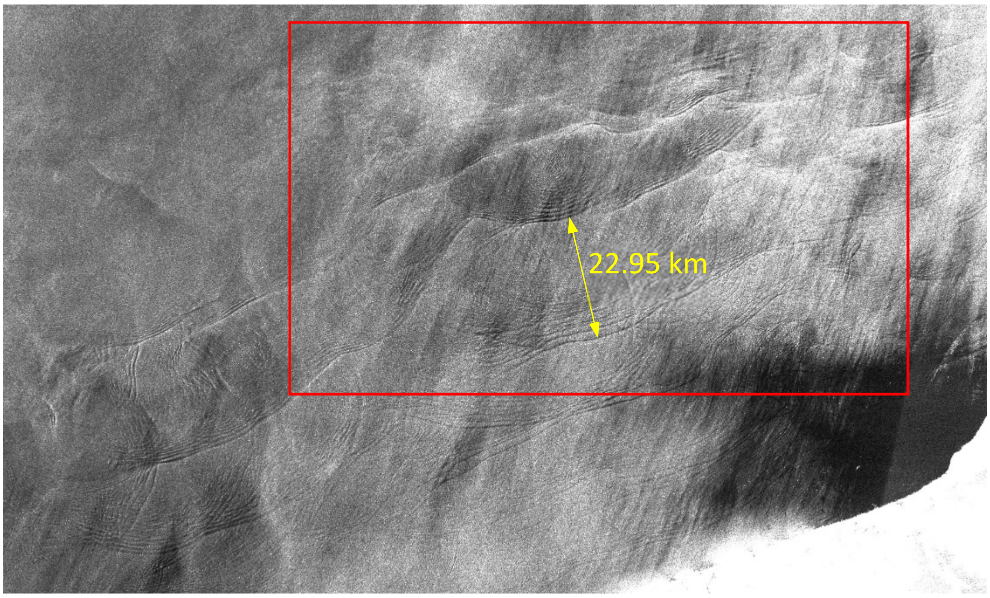

Figure 14. Rectangular zoom of the area shown in figure 13.
(Grey scaling: [0, 0.03])

From figure 14 the distance between two successive packages is nearly 23 km. Considering every package formed by a tidal movement and the period of main component of the tides in the area (M_2: 12.42 h) we can calculate the speed of the package performing a simple division, resulting in roughly 0.5 m/s. Finally, figure 15 shows the wavelength of the first crests in a package: it is close to 2 km. The individual waves traveling behind present decreasing distances between them, as expected.

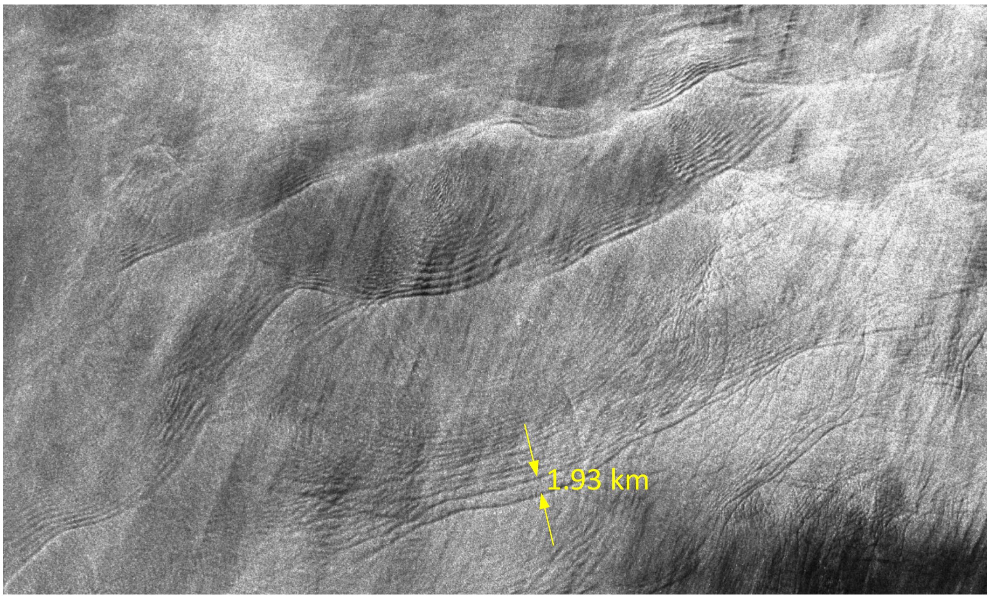

Figure 15. Rectangular zoom of the zoomed area shown in figure 14.
(Grey scaling: [0, 0.03])

4.1.3. Eddies

Small-scale structures as the eddies imaged in figure 16 are visible due to the accumulation of surfactants originated by the primary producers in convergence zones.

The anticyclonic eddy shown at northwest present a diameter of about 125 km, while diameter of the cyclonic is about 40 km. The formation of these structures, in particular, is related to the von Karman streets associated with La Palma and La Gomera islands.

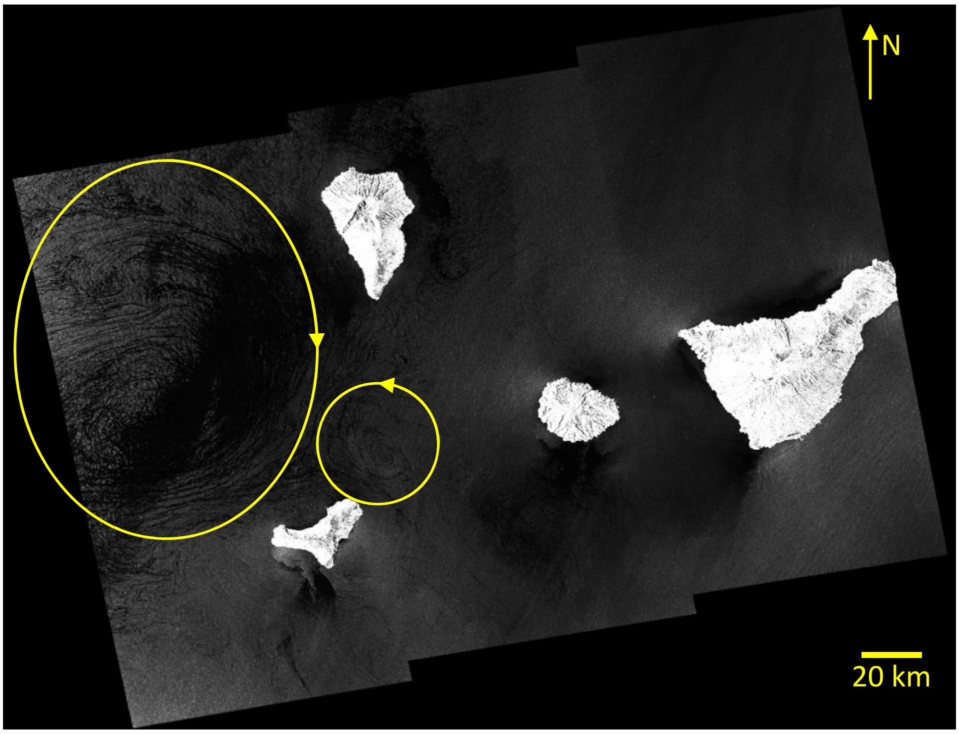

Figure 16. SAR image captured on October 11th, 2017. Eddies.

4.2. Air-Sea interactions

These four patterns (surface winds, roll vortices, gravity waves, and rain cells) are very frequent in our region.

4.2.1. Windrows or roll vortices.

The first very common air–sea interaction observed in our oceanic region is the formation of windrows (also called roll vortices). This class of interactions include phenomena such as gusty, sporadic low winds to windrows indicative of strong winds and from rain cells to hurricanes. All of them are difficult to analyse.

We have already seen windrows in figure 9. These structures are described, [3], as '*organized counterrotating secondary circulations, embedded in the mean flow, that result from instabilities in the convective marine boundary layer*'. The axis of these structures is parallel to the strong wind direction, and the corresponding wavelength ranges in the interval [1, 5] km, but may grow up to 15 km. The alternating SAR backscattering patterns are related to fluctuations in along-wind velocity within the near-surface convergent or divergence regions. In figure 17 we can see a schematic of roll vortices, at the top of it the 'rolls' are placed along the shear vector between the surface and geostrophic wind. The brighter bands are related to the convergence lines, while the dark lines corresponds to a vertical circulation. In the middle of the figure, the variation of the vertical component U_z of the wind velocity along the y direction is illustrated. At the bottom the variation of the horizontal components U_x and U_y (in the x, y plane) is represented.

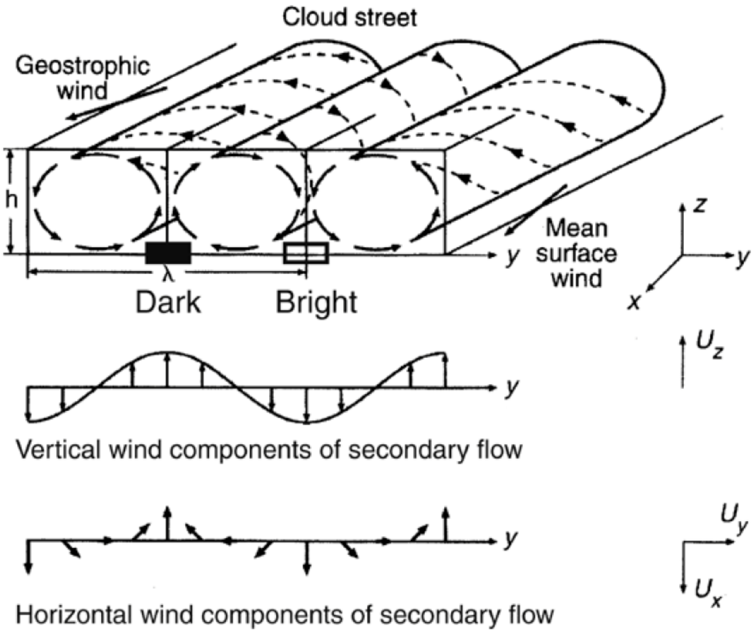

Figure 17. Model for the formation of roll vortices (from [3]).

The image in figure 18 is the well-known wind velocity field in our area, corresponding to June 30th, 2017. That day the wind was intense. In particular, near the coast of Africa, the speed was higher than 10 m/s, on the average.

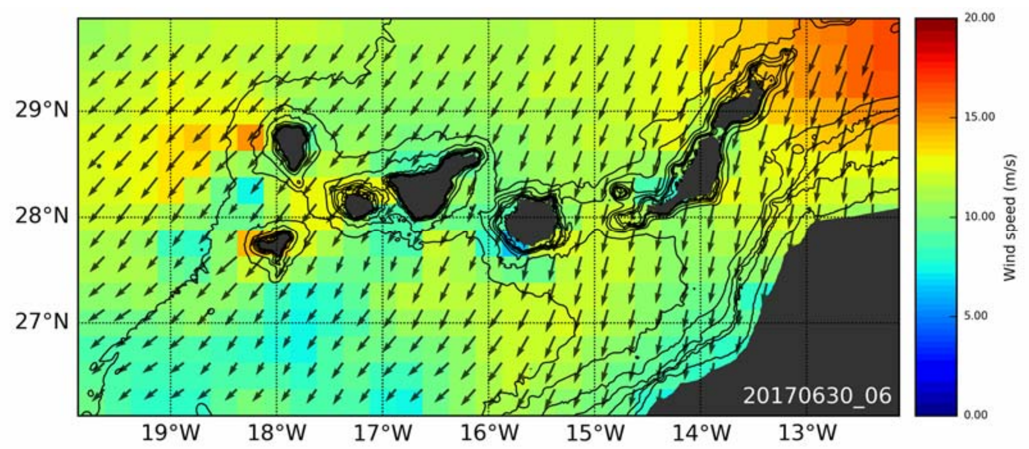

Figure 18. Average wind velocity field in the area on June 30th, 2017 at 6:00 AM.

Figure 19 illustrates a SAR image in which we can observe windrows all over the oceanic waters. In particular, we highlight an area where the pattern is quite regular.

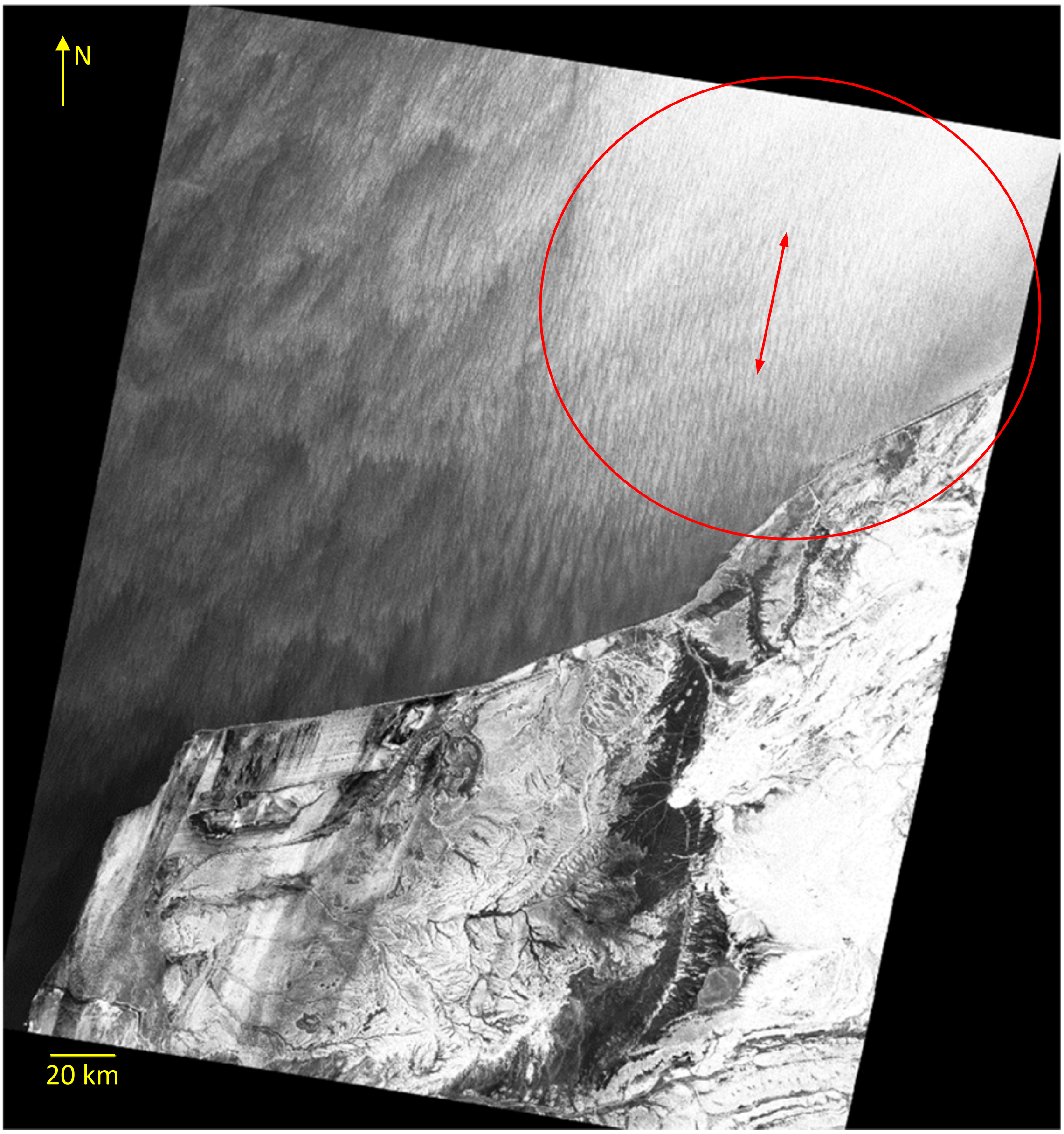

Figure 19. SAR image captured on June 30th, 2017. Roll vortices.

We have measured the average wavelength in the encircled area using SNAP, our results are a parameter close to 1.2 km.

4.2.2. Rain cells.

Figure 20 depicts a SAR image taken on March 18th, 2017. It contains many small rain cells, some are encircled in yellow, but others not. The cells are grey circular structures with the texture of a cotton ball in different sizes. In our region, they tend to be of about 10 km in diameter, or less, but they can reach 40 km. Those cells where it was raining at the time the image was captured (07:01 AM) present a brighter core (in C-band). The impacts between the falling drops and the surface of the ocean is responsible for the increase in brightness. In [11] they report estimations of rain intensity from SAR images.

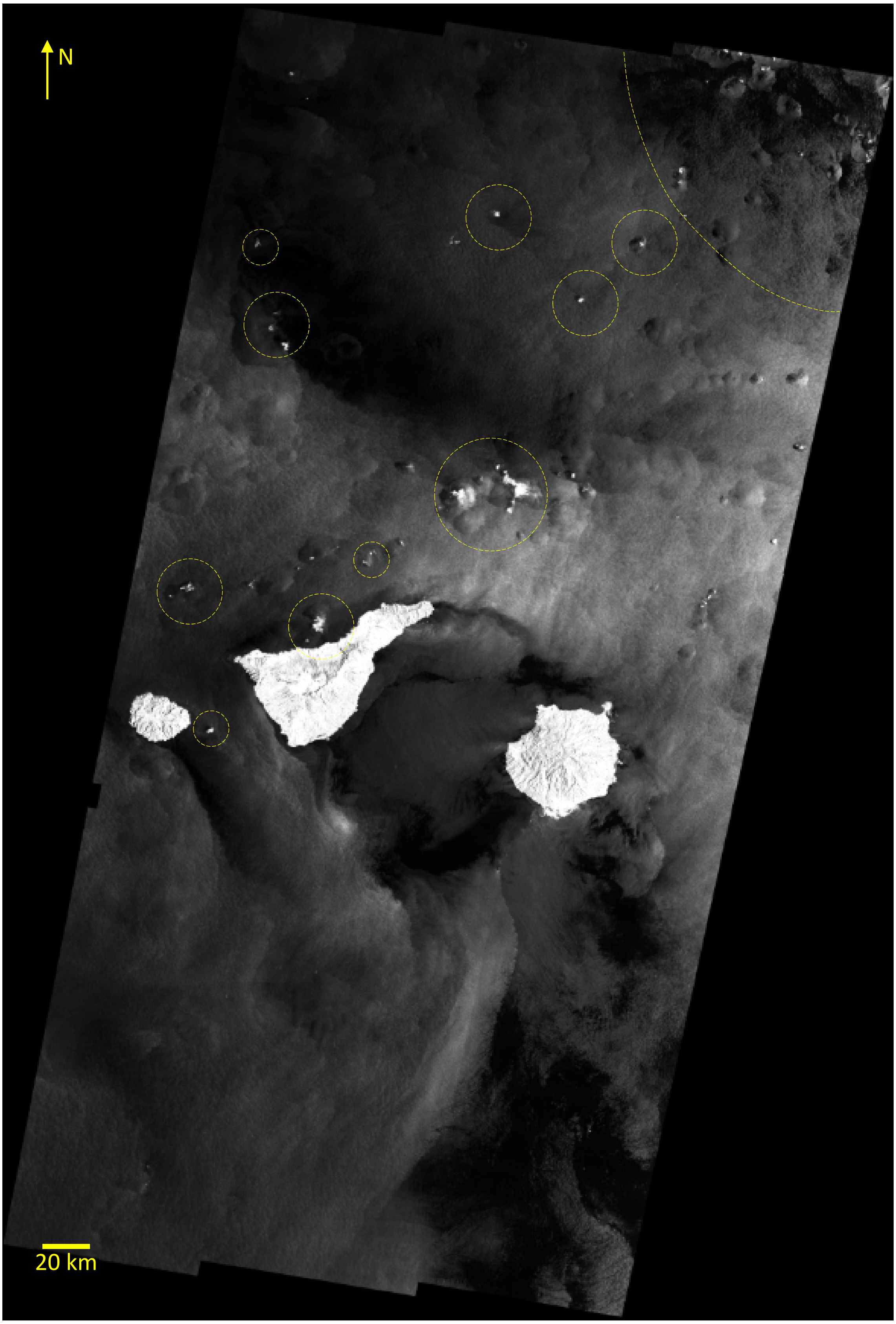

Figure 20. SAR image captured on March 18th, 2017. Rain cells.

4.2.3. Atmospheric gravity waves

When an atmosphere stratified and stable is perturbed (usually by a topographic feature, for example), downstream from the topographic feature atmospheric gravity waves appear. These waves present crests perpendicular to the wind velocity. They propagate in the same direction as the wind; and rotate about 18º clockwise in the northern hemisphere.

On the SAR image from July 13th in figure 21, the blue rectangles highlight atmospheric gravity waves. The topography of Tenerife is responsible for the formation of these waves. Note that this structure also appears twice in the channel between Tenerife and La Gomera. This image offers even more recognizable patterns. We have used double head arrows to mark windrows. Finally, the northeast of the image presents convective cells. Note also the von Karman streets at the southwest.

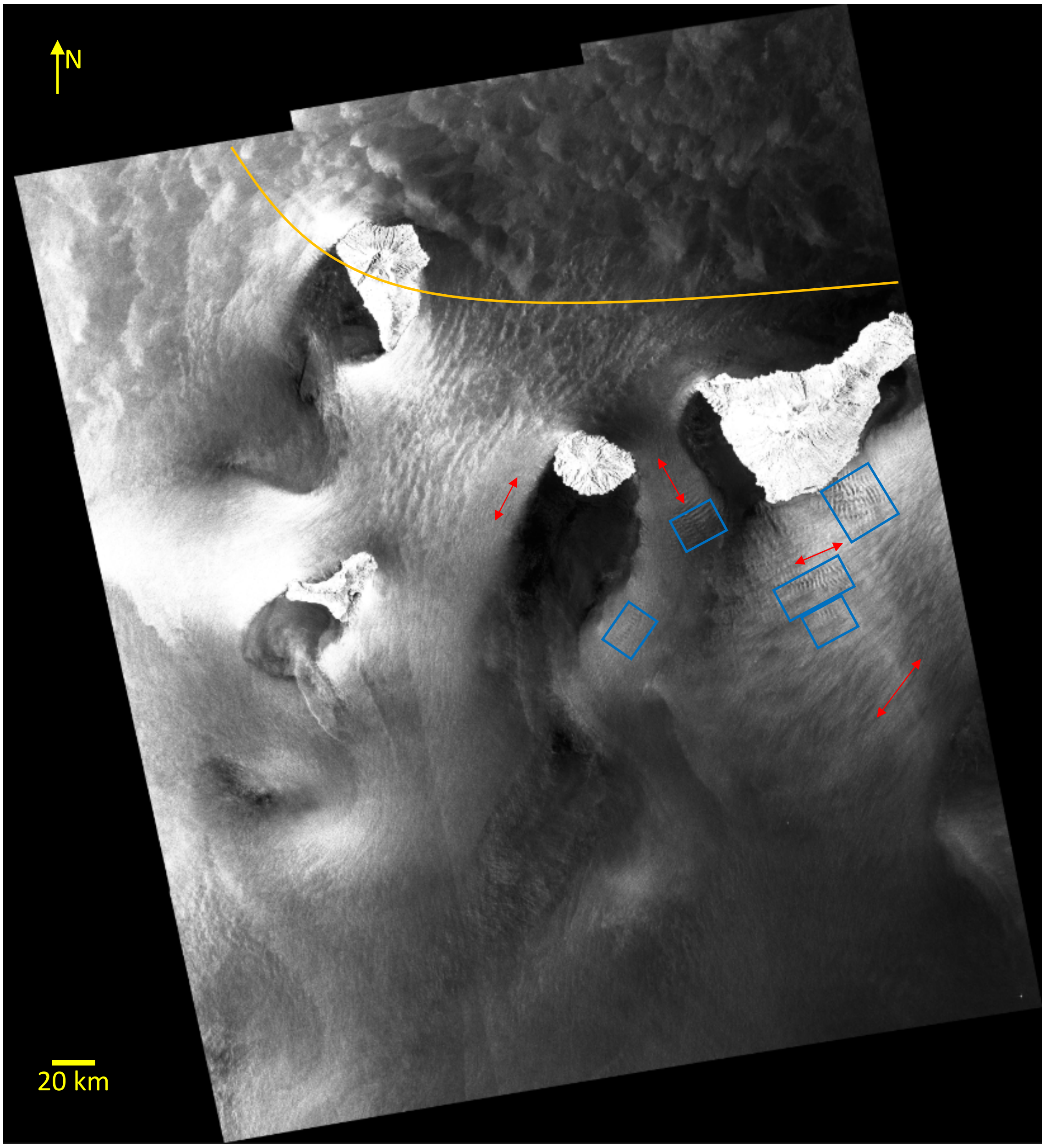

Figure 21. SAR image from July 13th, 2017.

It his instructive to devote some more time to this image observing figure 22. It is funny (peculiar) to find images from a visible radiometric sensor fitting so well with the corresponding SAR image because this only happens when sunlight is present and there is specular reflection. The visible image corresponds to sensor MODIS aboard satellite Aqua, it was captured the same day as the previous image.

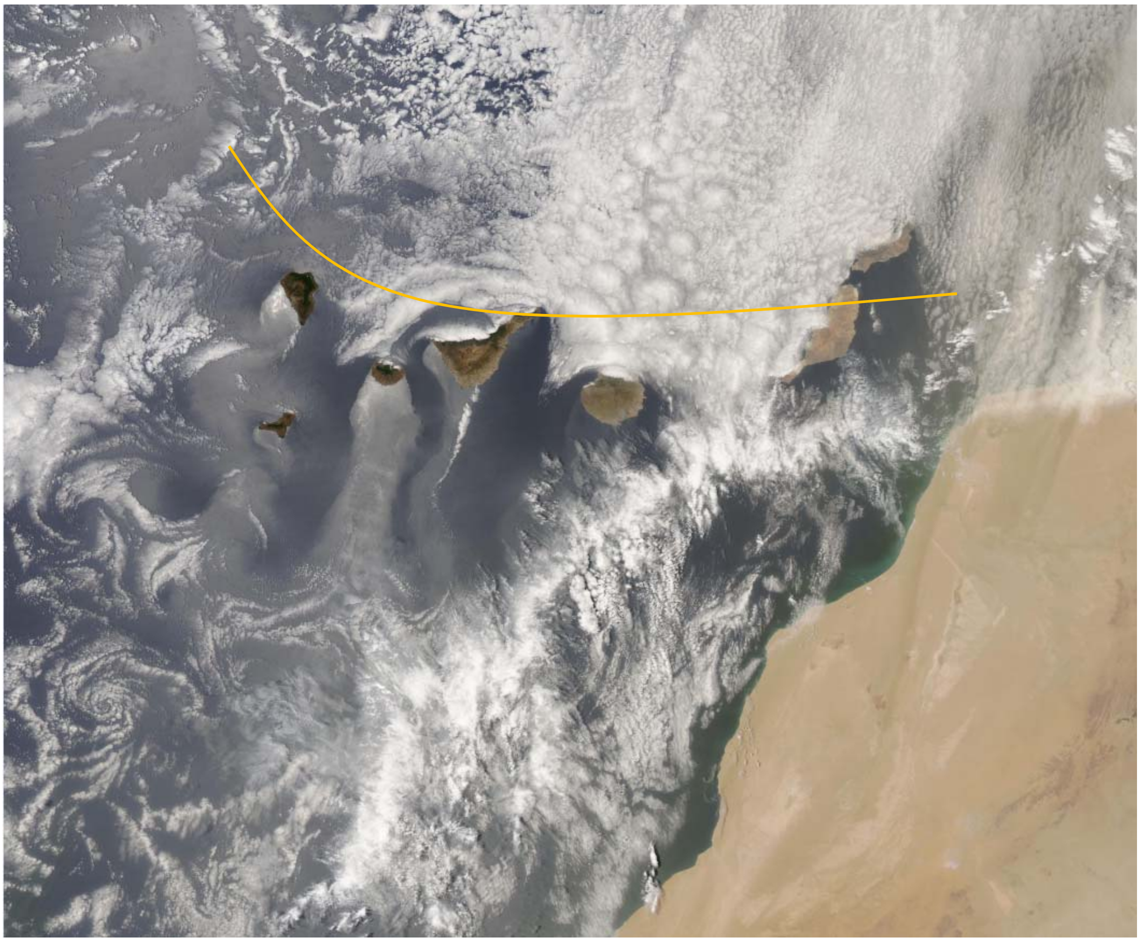

Figure 22. MODIS visible image from July 13th, 2017. (A few hours later than figure 21)

It is easy to appreciate the channel between Tenerife and La Gomera because the wind has swept the cloud cover. It is also noticeable the von Karman streets in the southwest. Moreover, zooming into this image we can see all the patterns highlighted in figure 21. Obviously, as long as we have pair of images like these ones (visible and SAR), the interpretation of the SAR image is greatly facilitated.

4.3. Surface films

In many SAR images, we can observe surface slicks whose origin is biogenic (natural and artificial) or mineral oils (natural and artificial –spills–). The slicks are usually seen better at smaller scales, so it is mandatory to zoom the image when looking for surface slicks.

Slicks are not new for us, they have already been observed in figure 16: in fact, we did not see eddies in the figure, what we saw were slicks modelled by the eddies.

4.3.1. Biogenic surfactants.

Figure 23 displays, encircled in yellow, a package of slicks at the north of La Gomera (and north of Tenerife) on April 10th. We can observe also some rain cells at the northwest. We will assume, in principle, that the origin of these slicks is natural because we do not have any other evidence.

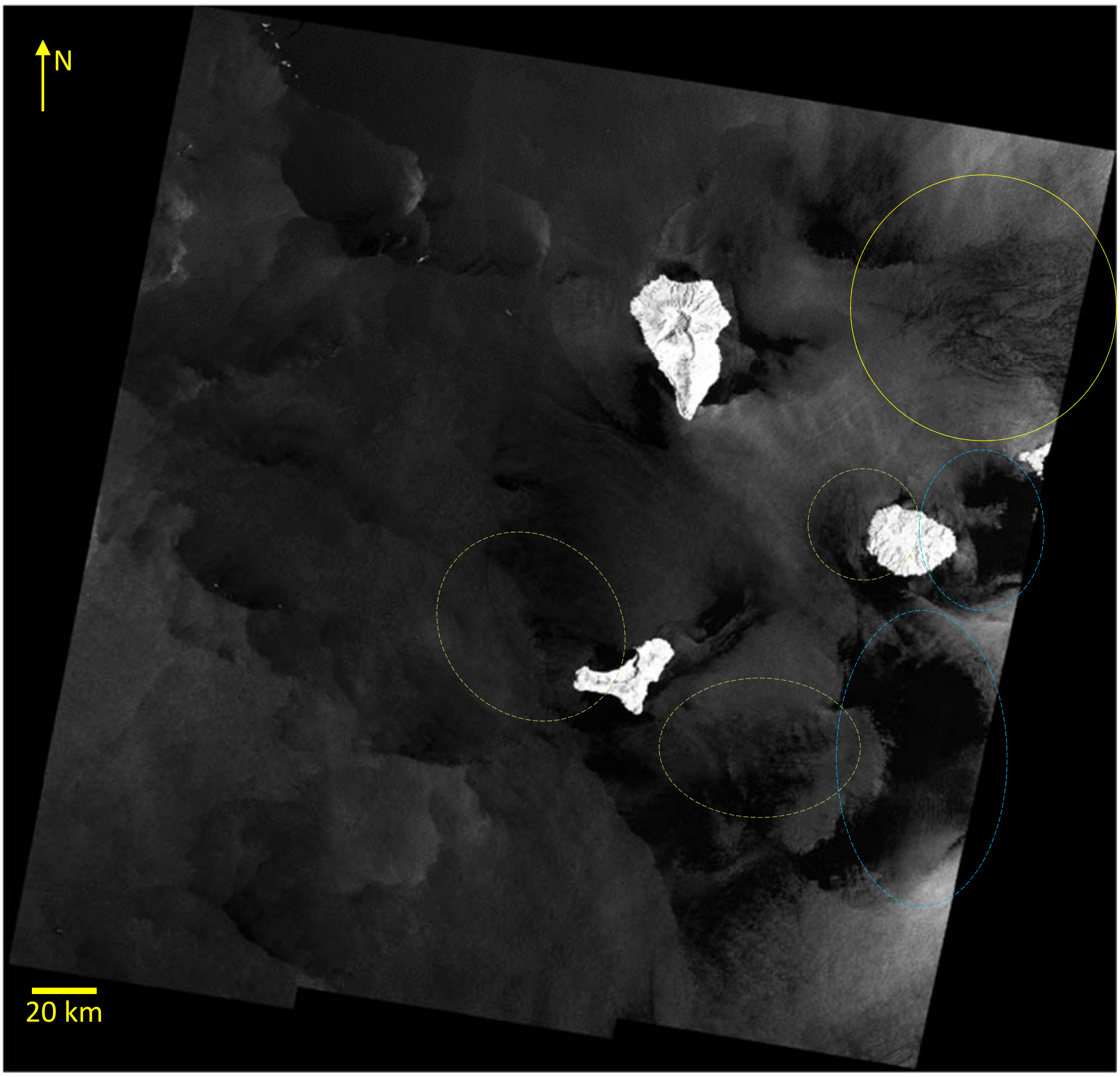

Figure 23. SAR image captured on April 10th, 2017. Biogenic surfactants (natural source).

To confirm this hypothesis figure 24 is incorporated. There we see the spatial distribution of chlorophyll-a concentration. Note the higher concentrations around La Gomera, and at the north of Tenerife, what is an indicative of primary producers in the area.

This SAR image has more slicks, allegedly natural, inside the green dashed circumferences in figure 23. The black areas highlighted by the blue ones do not backscatter any signal: this is usually due to a very low wind speed in that area; in such a way that the speed lower bound is not exceeded and no roughness is detected.

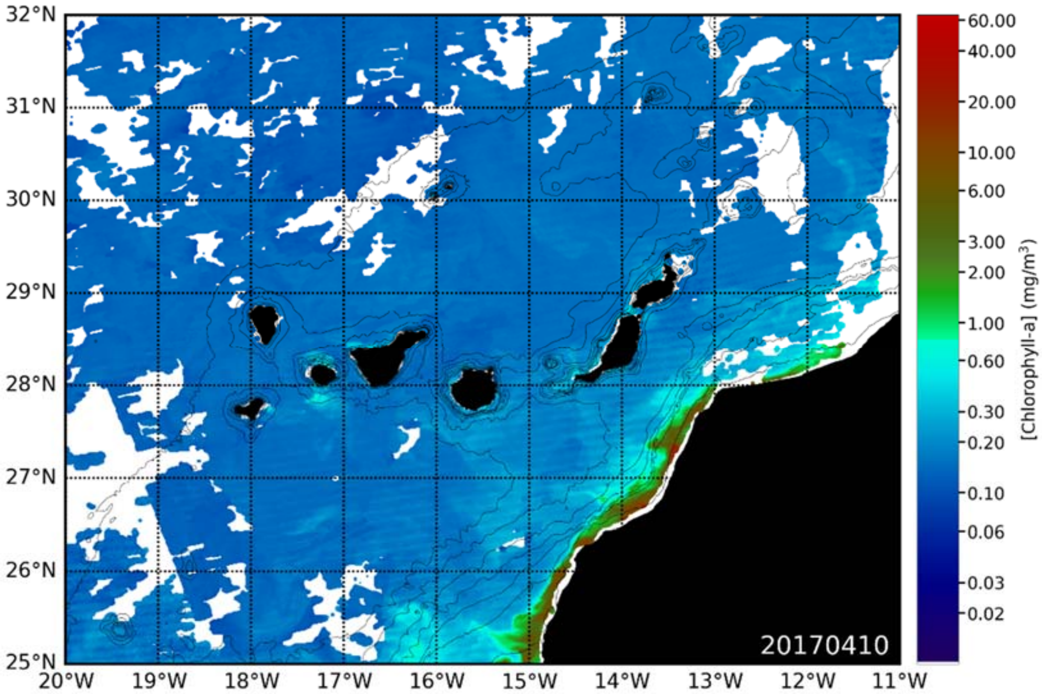

Figure 24. Chlorophyll-a concentration averaged for five days around April 10th, 2017.

Conversely, Figure 25, dated February 16th, illustrates an example of artificial slicks. There is a fish farm within the yellow circumference. The waste is responsible for the organic surfactant film. In addition, in the highly populated northeast coast many of the observed dark areas are spills of organic material (controlled or not).

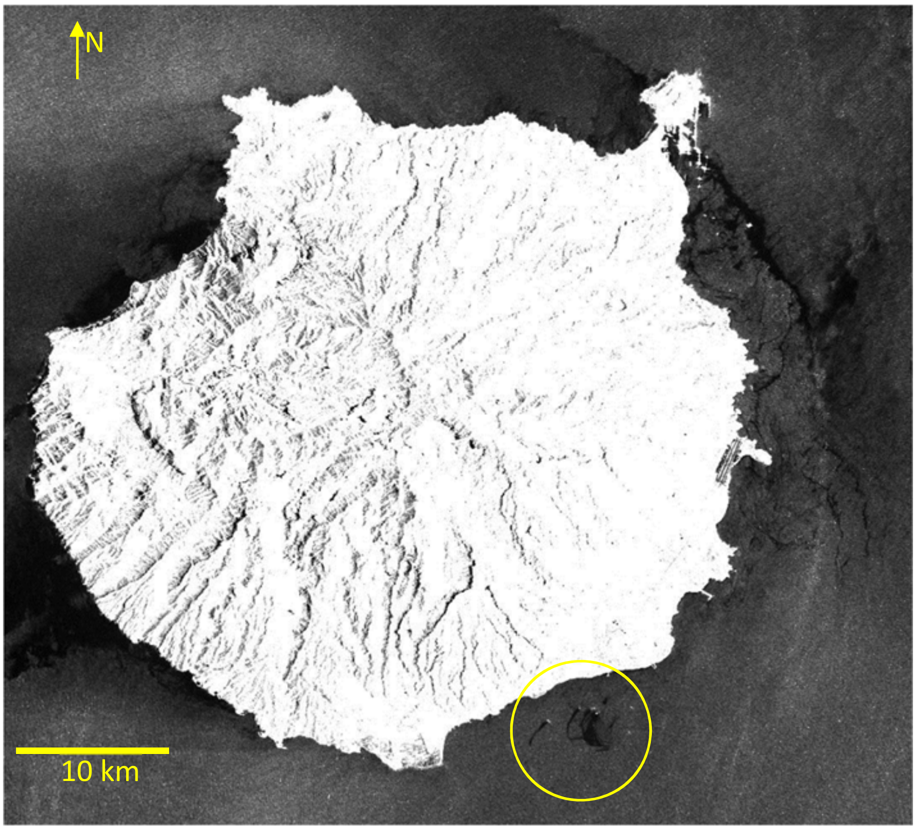

Figure 25. SAR image captured on February 16th, 2017. Biogenic surfactants (artificial source).

4.3.2. Oil stains.

An example of an artificial mineral slick is presented inside the yellow circumference laid-out in figure 26 that shows a SAR image captured on October 25th.

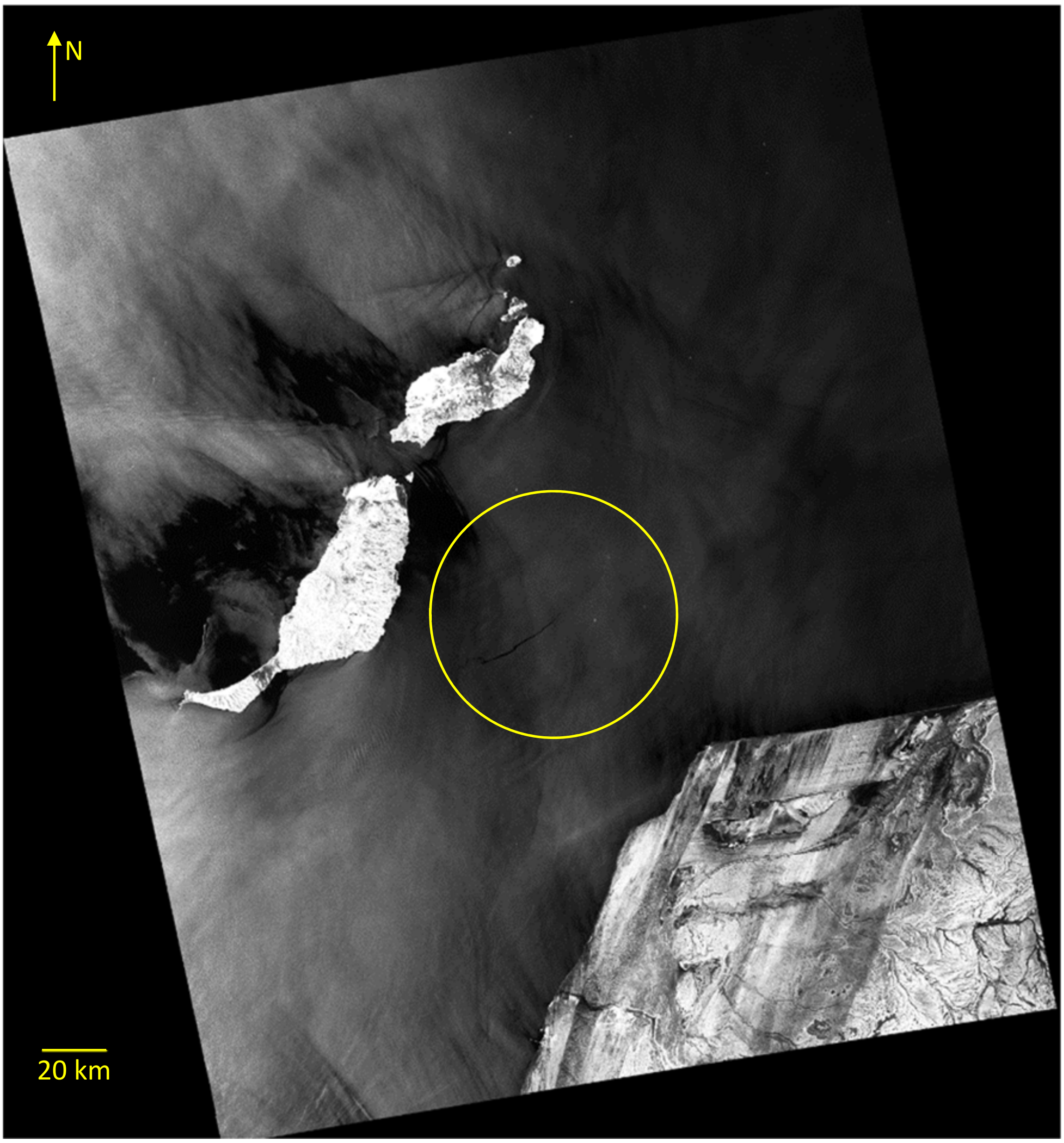

Figure 26. SAR image captured on October 25th, 2017. 4.9. Oil stains.

There are two ships and two spills in the yellow circumference. This can be better viewed in figure 27 where we have zoomed the area. The bright dots are the positions of two ships at the time the zone was imaged. The vessel labelled “Ship no. 2” is responsible for the spill: a first stain close to a length of 40 km and a second 9 km one. This has been produced for a period of time lasting a few hours, and it will persist there for a few more (even days, depending on weather and sea conditions). As far as the maritime authorities have record and tracks of the ships in transit through the area, it is possible to use SAR images as a surveillance system against this harm.

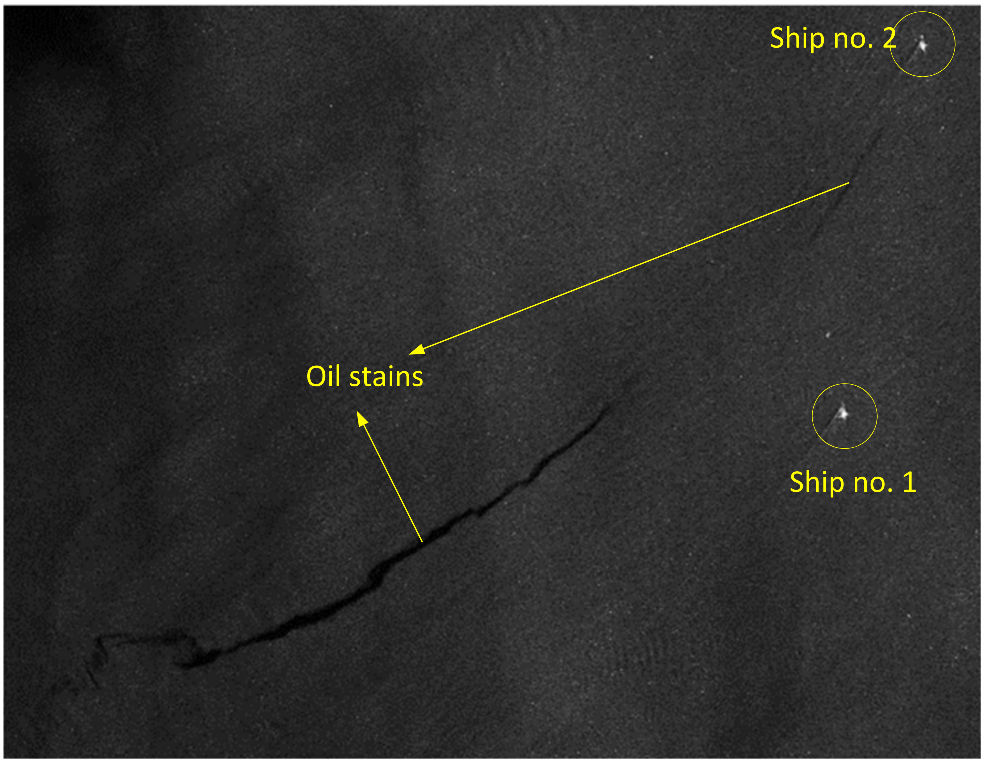

Figure 27. Zoom of the encircled area in figure 26.

Oleg Naydenov fire, sinking and spill

On April 2015, the media reported massively about the fire and sinking of a fishing boat called Oleg Naydenov on the south coast of Gran Canaria. The ship was plenty of oil at the time of its sinking. Once on the seabed, the Spanish authorities sealed the ship in order to stop the continuous spill of oil, costing around 80 M€. Figures 28 and 29 demonstrate, by means of SAR images, that in 2017 the oil was still escaping.

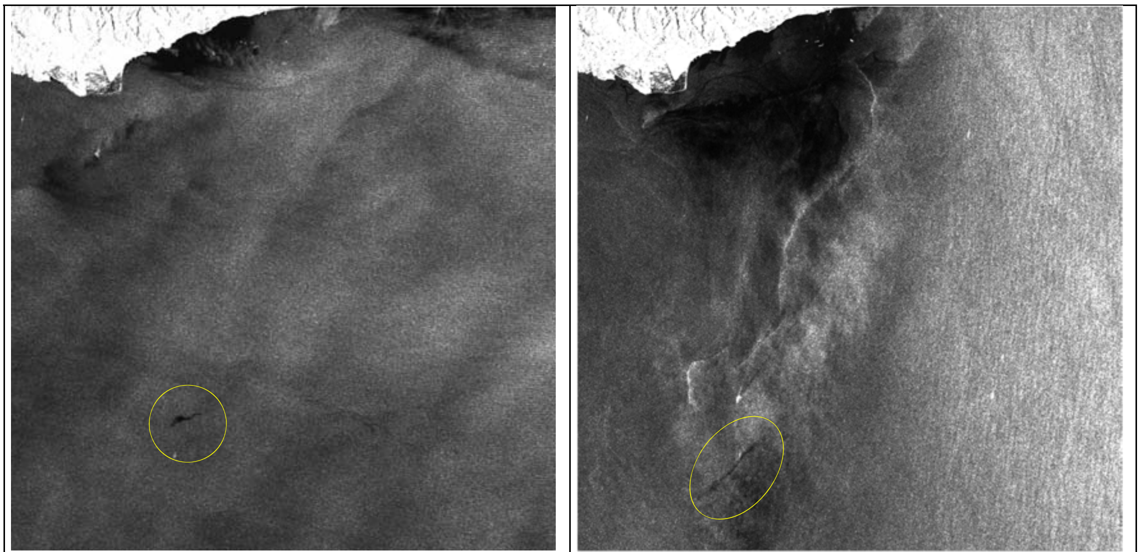

A B

Figure 28. SAR images from Gran Canaria southern coast in 2017. (A) April 29^{t}. (B) May 17th

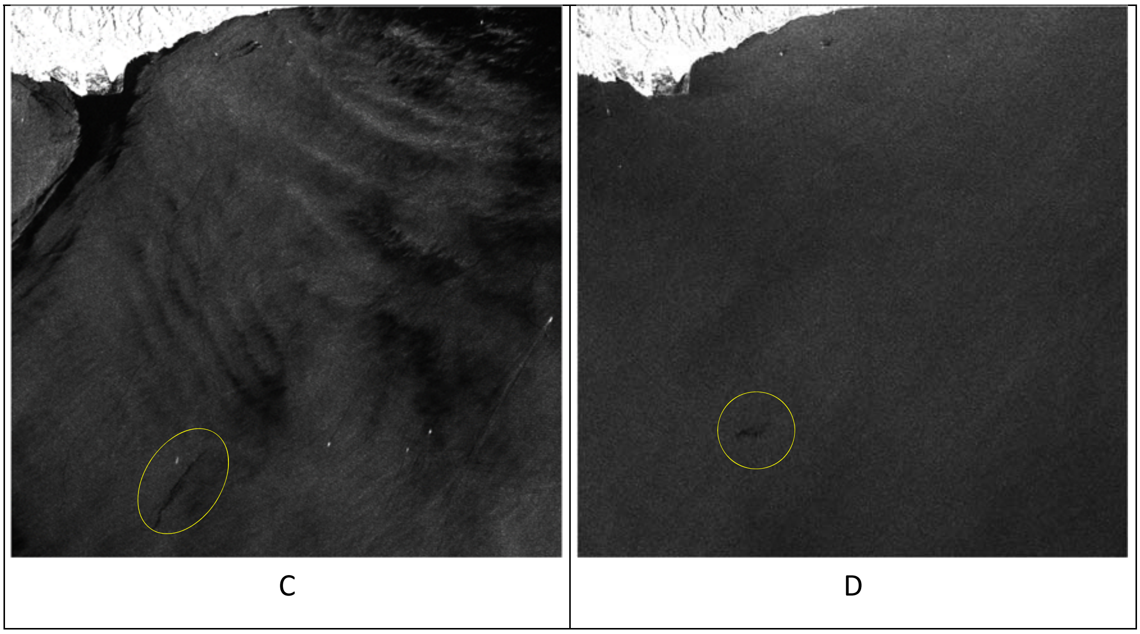

Figure 29. SAR images from Gran Canaria southern coast in 2017. (C) October 14^{th}. (D) November 23^{th}

4.4. Ship wakes.

Figure 30, from February 14^{th}, shows a rare situation. Note how are visible the wakes of two ships travelling between Gran Canaria and Tenerife. The covered distance is about 65 km, and the trip lasts about 90 minutes. The propellers perturb water to produce that signal.

If we look carefully many of the previous SAR images, we would see many ship wakes.

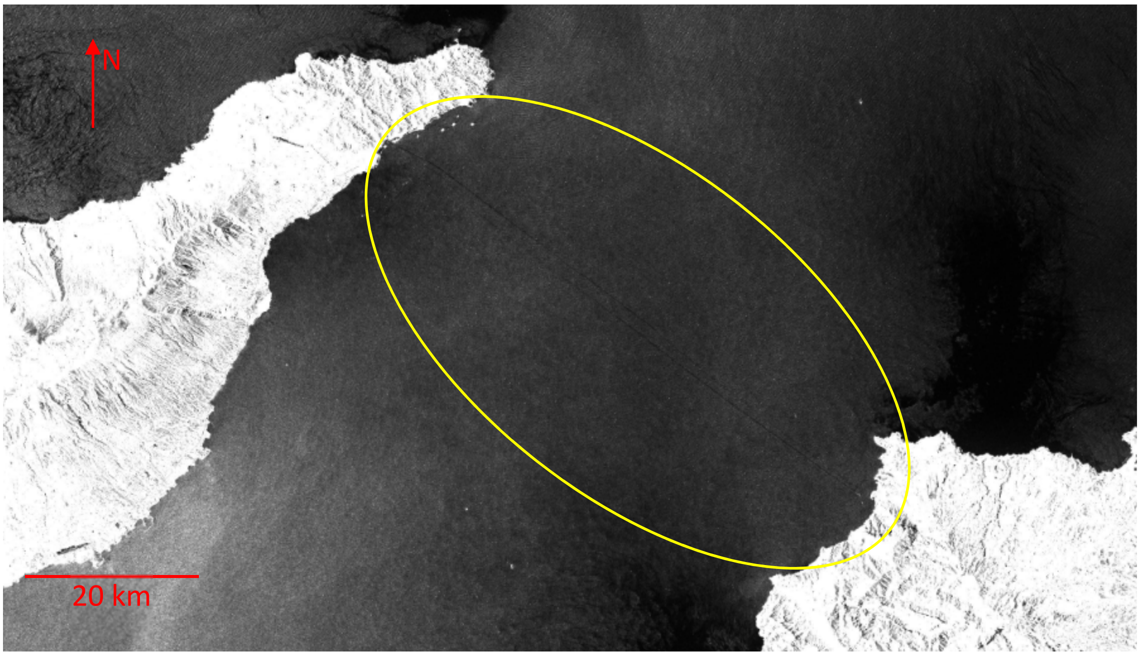

Figure 30. SAR image captured on February 14^{th}, 2017. Ship wakes.

5. Conclusions

Oceanic Synthetic Aperture Radar images are a tool capable of providing information on a variety of phenomena such as '*internal waves, currents, upwelling, shoals, sea ice, wind, and rainfall*', [3]. Nevertheless, in this document we have illustrated that it is far from easy to interpret what are the physical, biological or chemical causes behind a particular pattern in the image. In some cases, there is more than one effect responsible for the same pattern. In other cases it is the combination of a number of causes what result in that pattern.

After a very basic statement of the basic principles on remote sensing with SAR, we mentioned the procedures needed to obtain useful images. However, not only the images are required to interpret them. We have exemplified that the so called environmental data are much needed to perform our task. This also requires procedures. Many of them.

At this point, it is worth mentioning some learning experiences of the candidate:

- To understand a SAR image it is required to read consciously some literature about fundamentals on SAR. We suggest [3] as a good starting point.
- It is mandatory to train the eyes. SAR is a new language and at the beginning of the process, a SAR image is simply a group of grey stains. You have to see many, many images to start recognizing some patterns and understanding the meaning.
- Of course, you also need to see quasi-true colour images. Without them no interpretation is conceivable.
- It is also important to maintain discussions with skilled people. The candidate have had the opportunity to review many images with:
  - The advisors: Francisco José Machín Jiménez and Josep Coca Sáenz de Albéniz,
  - Some professors: Antonio Juan González Ramos, Ángel Rodríguez Santana, and Luis García Weill, and
  - A researcher: Samuel Hormazábal Fritz.

As concluding remarks, we can summarize our achievements as follows:

- We have been carrying some basic research work done in the field of interpretation of imagery taken from C-SAR sensor aboard of Sentinel-1 satellites in the oceanic waters bathing Canary Islands.
- We have acquired a basic knowledge of SAR instrumentation mounted on Sentinel-1 satellites, and on interpreting SAR images.
- We have been working with SAR images of the year 2017 in the oceanic region of interest.

- We have identified most of the more frequent patterns encountered in the region. That knowledge has been summarized as a guide to facilitate the interpretation of upcoming new images.
- We have suggested applications of this technology: development of surveillance platform for marine pollution events. In fact, there is a H2020 research project called Impressive[19], in which our University is a partner. The project leader in ULPGC is Dr. Antonio Juan González Ramos, who has been supporting the candidate during the development of the work.
- There are more applications of SAR imagery that has been already mentioned like tracking ships or floats, or surveillance of meteorological events.

An additional remarkable conclusion: we have learned that, at least in our oceanic region, **atmospheric stability** greatly constrains the observability of phenomenon.

At the beginning of the work, the candidate knew nothing about SAR, now he treasures some little knowledge about it. Nevertheless, the perception of ignorance remains. The foundations for that feeling is this last image…

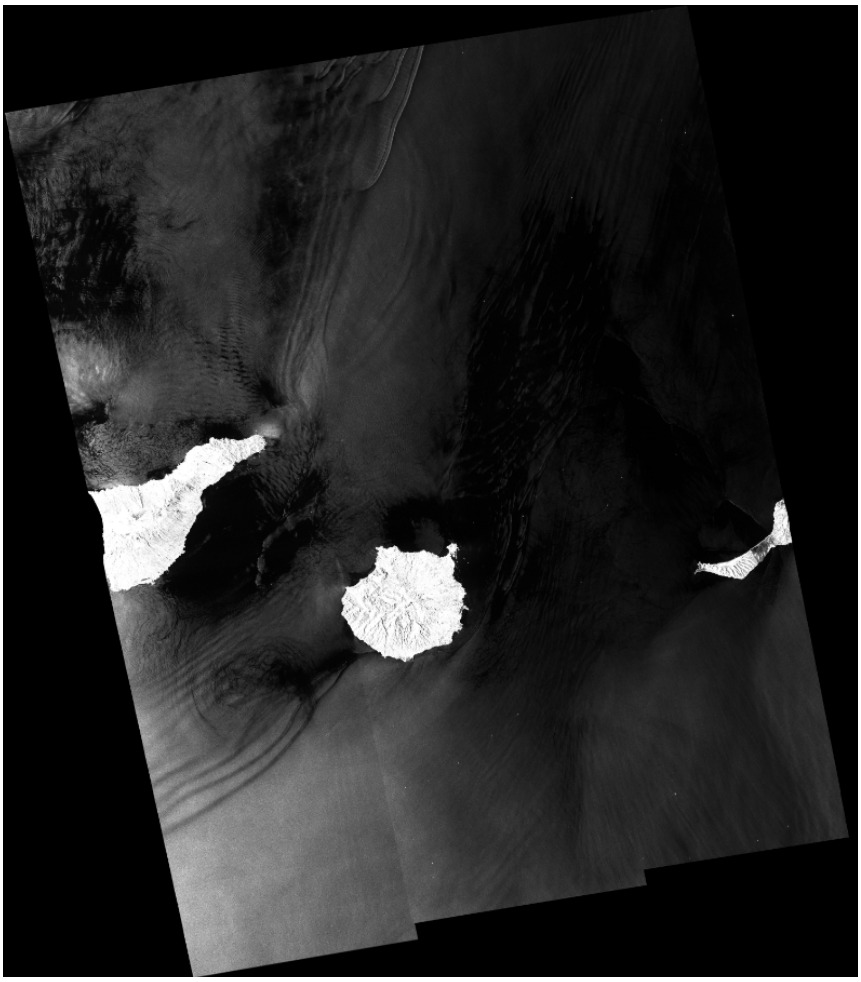

We wonder if someone is able to explain everything observed here.

[19] http://impressive-project.eu/

6. References

[1] http://www.esa.int/Our_Activities/Observing_the_Earth/Copernicus (visited June 2019)

[2] https://www.copernicus.eu/en (visited June 2019)

[3] Jackson, C.R. and Apel, J.R. (editors). *Synthetic Aperture Radar Marine User's Manual*. U.S. Department of Commerce, National Oceanic and Atmosferic Administration. 2005: http://www.sarusersmanual.com/ (visited June 2019)

[4] Link to download SNAP: https://bit.ly/2VFlFTU (visited June 2019)

[5] Olmsted, C. *Scientific SAR User's Guide*. Alaska SAR Facility. Geophysical Institute of the University of Alaska Fairbanks. 1993. https://bit.ly/2Lcapsu (visited June 2019)

[6] https://bit.ly/2Kr1gMn (visited June 2019)

[7] Jensen, J.R. (2000) Remote Sensing of the Environment: An Earth Resource Perspective. Prentice Hall, Saddle River.

[8] European Space Agency, Sentinel-1 Product Definition. Document Number: S1-RS-MDA-52-7440. https://bit.ly/30s8QdJ (visited June 2019)

[9] https://pypi.org/project/sentinelsat/ (visited June 2019)

[10] 8th ESA Training Course on Radar and Optical Remote Sensing. Institute for Environmental Solutions (IES), Cesis, Latvia (2016): https://bit.ly/30ofvWV (visited June 2019)

[11] Melsheimer, C., W. Alpers, and M. Gade, "Simultaneous observations of rain cells over the ocean by the synthetic aperture radar aboard the ERS satellites and by surface-based weather radars." *J. Geophys. Res.*, 106 (C3), pp. 4665–4677. 2001

7. Annex I. List of acronyms

ASCAT: **A**dvanced **SCAT**terometer.

ECMWF: **E**uropean **C**entre for **M**edium **W**eather **F**orecasts.

EOSDIS: **E**arth **O**bserving **S**ystem **D**ata and **I**nformation **S**ystem.

ESA: **E**uropean **S**pace **A**gency.

EUMETSAT: **Eu**ropean Organisation for the Exploitation of **Met**eorological **Sat**ellites.

GIBS: **G**lobal **I**magery **B**rowse **S**ervices.

MODIS: **MOD**erate resolution **I**maging **S**pectroradiometer.

NASA: **N**ational **A**eronautics and **S**pace **A**dministration.

NOAA: United States **N**ational **O**ceanic and **A**tmospheric **A**dministration.

RADAR: **RA**dio **D**etection **A**nd **R**anging.

SAR: **S**ynthetic **A**perture **R**adar.

SST: **S**ea **S**urface **T**emperature.

SUOMI-NPP: **Suomi N**ational **P**olar-orbiting **P**artnership.

VIIRS: **V**isible **I**nfrared **I**maging **R**adiometer **S**uite.

8. Anexo II. Cuestionario

8.1. Descripción detallada de las actividades desarrolladas

Si bien en algunas asignaturas del Grado en Ciencias de Mar se abordan aspectos relacionados con la detección vía satélite, especialmente en el visible, ninguna de las asignaturas trata de imágenes radar y su interpretación, específicamente. De modo que es preciso complementar la formación adquirida en los estudios de Grado para abordar una introducción a los conceptos básicos de teledetección con SAR. Con posterioridad se abordan temas de interpretación de las imágenes en una región geográfica concreta seleccionada por los tutores, a saber: todo el archipiélago canario como imagen sinóptica de conjunto, y del litoral de la isla de Gran Canaria, en particular, como zona particular de análisis.

Como herramienta de interpretación se utiliza el programa SNAP, acrónimo de *Sentinel Application Platform*, un software gratuito de la ESA concebido para procesar y analizar las imágenes captadas por la constelación de satélites Sentinel–1.

Con todo, las actividades más relevantes que han sido desarrolladas durante este periodo son las siguientes:

- Recopilación y lectura de información relevante sobre teledetección con SAR.
  Esta tarea se desglosa en: visitas a la biblioteca de Ciencias Básicas, búsquedas en internet, recepción de información aportada por los tutores y lectura de documentos seleccionados.
- Manejo del software de procesamiento de imágenes de teledetección, SNAP.
  Visualización y procesado de imágenes SAR mediante el programa SNAP. Dicho programa está preinstalado en el sistema informático disponible en el laboratorio.
- Interpretación de imágenes SAR.
  Para la realización de esta tarea se requieren las siguientes herramientas:
  - una completa base de datos de imágenes de Sentinel 1 del año 2017, y de otra información accesoria que más adelante se detalla,
  - el texto de la NOAA titulado "*Synthetic Aperture Radar Marine User's Manual*" y
  - el software de procesamiento SNAP.

El análisis de las imágenes ha permitido elaborar un "catálogo" de las estructuras más frecuentes en el entorno del archipiélago canario.

8.2. Formación recibida (cursos, programas informáticos, etc.)

Manejo del software de procesamiento de imágenes de teledetección, SNAP. Ya se ha indicado que este paquete software de código abierto es ofrecido por la ESA. SNAP presenta numerosos "*Toolboxes*" con los que comparte arquitectura. Se trata de una herramienta válida para la explotación de datos de observación de la Tierra.

A nivel de usuario SNAP facilita la interpretación de las imágenes gracias a su capacidad de georrefenciación y, con ello, la posibilidad de medir longitudes de onda de fenómenos oceanográficos. Estas medidas permiten caracterizar algunos de los fenómenos de interés.

Por otro lado, al carecer de conocimientos básicos de SAR imprescindibles, al tratarse de una temática nueva, ha sido necesario adquirir la formación básica sobre esta tecnología (teledetección con SAR) y sus fundamentos físicos.

8.3. Nivel de integración e implicación dentro del departamento y relaciones con el personal.

La acogida en el grupo de trabajo ha sido excelente, de modo que el estudiante se ha sentido integrado desde el principio. Por otro lado, los tutores han respondido con diligencia a las cuestiones planteadas, facilitando su tarea en buena medida.

8.4. Aspectos positivos y negativos más significativos relacionados con el desarrollo del TFT

Quien suscribe está bastante satisfecho con el tema (si bien resulta un tanto árido en parte de su desarrollo), con el equipamiento puesto a su disposición y, sobre todo, con el trato personal recibido.

Aspectos negativos prácticamente ninguno, si acaso alguna carencia del edificio que no cabe señalar aquí.

8.5. Valoración personal del aprendizaje conseguido a lo largo del TFT.

Conforme a lo recogido en el párrafo anterior la valoración personal es muy positiva. Se trataba de un campo nuevo para el estudiante: una especie de nuevo lenguaje que, con suficiente entrenamiento, poco a poco, se va conformando en un nuevo canal de comunicación con la naturaleza.